Modelling of Biomass Pyrolysis with Ex-situ Catalytic Upgrading for Bio-crude Production

Febryana Nugrahany

School of Engineering

Master's thesis
Espoo 25.5.2018

Supervisor

Prof. Mika Järvinen

Advisor

Weihong Yang, PhD
Henry Persson, MSc

Aalto University
School of Engineering

Author Febryana Nugrahany

Title of thesis Modelling of Biomass Pyrolysis with Ex-situ Catalytic Upgrading for Bio-crude Production

Master programme Innovative Sustainable Energy Engineering

Thesis supervisor Prof. Mika Järvinen

Thesis advisor(s) Weihong Yang, Henry Persson

Date 25.05.2018 **Number of pages** 52 **Language** English

Abstract

This study presents a techno-economic assessment of slow pyrolysis of pine sawdust continued by ex-situ catalytic upgrading. The overall process consists of six sections: feed drying, pyrolysis, vapor filtration, ex-situ catalytic upgrading, vapor quenching, and combustion of permanent gas. In the process simulation, biomass is objected to slow pyrolysis at 450ºC in an electrically-heated screw reactor and pyrolysis vapors is upgraded in fixed catalytic bed reactor at 425 ºC (using HZSM-5). The model is then used to investigate effects of feed moisture variation and type of heating source in pyrolysis unit, i.e. thermal vs. electrical heating, to oil energy efficiency. According to the simulation model, the endothermic pyrolysis step requires 1.46 MJ/kg dry-feed. On the other hand, ex-situ upgrading is slightly exothermic and releases 50kJ/kg dry-feed. Overall, the conversion of biomass to bio-oil demonstrates a mass efficiency of 19.65%wt and an energy efficiency of 29.10%. The energy efficiency raises to 32.81% if direct thermal source is applied instead of electrical heating. The bio-oil energy efficiency increases by 1.38% if the moisture content of the biomass decreases by 10%wt. In average, bio-oil and char production in ex-situ catalytic upgrading generates profit 1.47 SEK/kg dry-feed. The uncertainty of bio-oil price causes the highest profit variation.

Keywords ex-situ catalytic upgrading, slow pyrolysis, screw pyrolyzer, fixed bed catalytic reactor, process design

GLOSSARY

CFP	: Catalytic Fast Pyrolysis
ESP	: Electrostatic Precipitator
FCC	: Fluid Catalytic Cracking
HFO	: Heavy Fraction Bio-oil
HGF	: Hot Gas Filter
HHV	: Higher Heating Value
HP	: Hydroprocessing
(H)ZSM-5	: Proton-exchanged Zeolite Socony Mobil-5
LFO	: Light Fraction Bio-Oil
MC	: Moisture Content
NCG	: Non-Condensable Gas
VOC	: Volatile Organic Content

TABLE OF CONTENT

LIST OF FIGURES

LIST OF TABLES

1 INTRODUCTION

Excessive exploitation of fossil fuel causes rapid depletion and heavily burdens the Environment. Such issues encourage the quest to find alternative pathways to produce energy and chemicals from sustainable resources. Biomass as the only carbon-containing renewable source is considered to be a promising alternative to substitute fossil fuel. Consequently, bio-oil as a biomass product derived from pyrolysis process gains increasing interest since it is easier to be transported. However, direct treatment of bio-oil in existing infrastructure for fuel and chemical production is still challenging due to its characteristics. Its high oxygen content results in poor quality such as high acidity, low chemical stability and heating value [1]. Therefore, upgrading process to remove oxygen content is essential for bio-oil vapors before quenching.

Catalytic Fast Pyrolysis (CFP) are one of the most common upgrading routes [2, 3, 4]. The configuration of CFP which resembles current oil refineries makes it easier to adapt. However, the formation of thermal and catalytic coke is the major issue associated with this technique [5]. Rapid coke formation in catalytic processing causes catalyst deactivation while frequent regeneration potentially shortens the catalyst lifetime due to the risk of sintering and ash poisoning [6].

As an alternative solution, ex-situ catalytic upgrading method is recently developed. In such method, the pyrolysis process and catalytic upgrading are separated into two units so char which contains most of ash can be removed before catalytic upgrading process. Hence, the risk of catalyst poisoning by ash reduces. A combination of an auger reactor for pyrolysis unit with fixed bed catalytic reactor is particularly attractive. A screw reactor for pyrolysis offers advantages such as low carrier gas flow, a possibility of the absence of heat carrier and flexibility of the biomass particle size [7] while a fixed bed catalytic reactor is more flexible to precious catalyst [8, 9] compare to the fluidized bed reactor. However, most studies are still in pilot scale and industrial scale plant is unavailable. So, a simulation tool is required to assess the performance of the overall industrial-scale system.

This study aims to simulate and evaluate a process of pyrolysis of biomass in a screw reactor with ex-situ catalytic upgrading of pyrolytic vapors in a fixed bed reactor. The mass and energy balance of each section, modelled via Aspen Plus, is thoroughly examined. All required data for simulation are based on literature review. Results are then compared to performances of existing technologies. Furthermore, the study also investigates the effect of the feedstock's moisture content on the energy efficiency of bio-oil. A simple economic analysis is addressed to understand the impact of price uncertainty. The report is organized into five chapter. Chapter 2 provides the basic concept of ex-situ vapor upgrading. Chapter 3 describes the process along with procedures related to data collection and developments of simulation in detail. Chapter 4 discusses the results obtained. Finally, chapter 5 concludes the work and enlisted recommendations for further studies.

2 LITERATURE STUDY

This chapter aims to briefly summarize all basic concepts related to the modelling of ex-situ upgrading. It covers the description of four vital topics: (1) pyrolysis type including bio-oil properties and the superiority of screw reactor, (2) vapor upgrading, including the comparison between ex-situ and in-situ as well as the benefits of fixed bed catalytic reactor, (3) pretreatment and separation process and (4) current experiments in ex-situ catalytic upgrading.

2.1 Pyrolysis

Pyrolysis is defined as a thermal decomposition process of biomass in an oxygen-free atmosphere. Pyrolysis yields three types of products, namely char, permanent gas, and condensable gas which can be condensed into bio-oil. Figure 1 visualized the reaction path of pyrolysis. Pyrolysis has been extensively studied, and most studies observed that pyrolysis is an endothermic reaction [[10, 9, 11].

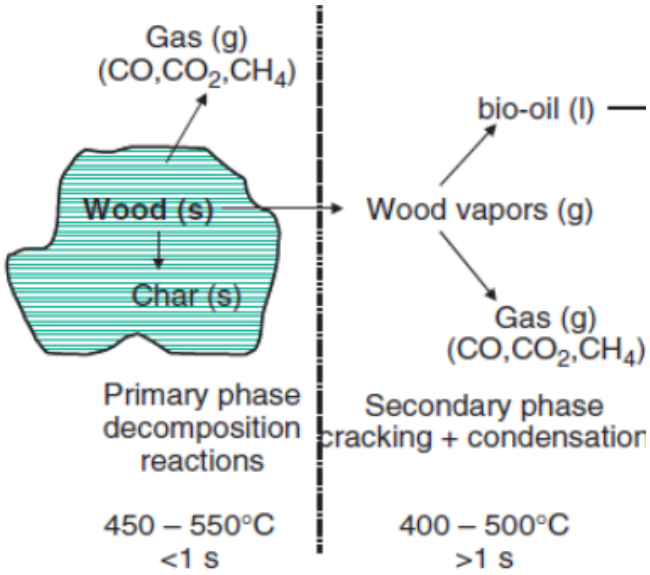

Figure 1 Reaction Path of Biomass Pyrolysis [12]

Depending on the operating conditions, mainly heating rate, pyrolysis is conventionally classified into three categories: slow, fast and flash as summarized in Table 1. Temperature also plays a crucial role in product distribution. A higher temperature leads into higher permanent gas yield while lower temperature limited the generation of pyrolysis vapor [13].

Table 1 Typical Operating Condition and Product Yield for Pyrolysis [14, 15]

Type	*Temperature (K)*	*Heating rate (T/s)*	*Solids residence Time (s)*	*Product Yield (% wt.)*		
				Liquid	*Solid*	*Gas*
Fast	850-1250	10-200	0.5-10	75	12	13
Flash	1050-1300	>1000	<0.5	50 (2 phases)	25	25
slow	550-950	0.1-1	450-550	30 (2 phases)	35	35

As presented in Table 1, slow pyrolysis possess a lower organic bio-oil yield than other two pyrolysis types due to secondary reaction. The combination of longer residence time and poor

heat transfer promoted a further devolatilization and dehydration of condensable intermediates [16].

2.1.1 Bio-oil

Among the three products of pyrolysis, bio-oil attracts the most attention due to its potential to partially replace fossil fuel [17] and its unstable properties. Unlike char which can readily be exploited subsequent to pyrolysis, bio-oil requires further treatment to upgrade its properties. Bio-oil is a complex multi-component mixture – normally water soluble and non-water soluble. It composes from about 300-400 compounds which are classified into six general categories: hydroxyaldehydes, hydroxyketones, sugars and dehydrosugars, carboxylic acids, and phenolic compounds [1]. High oxygenates content of bio-oil i.e. 35-40 %wt. [18] possibly lead to a further aging reaction during the storage of pyrolysis oil [12]. A stable bio-oil is characterized by low oxygen content and certain types of remaining oxygenates species. For instance, acid, aldehydes and ketones are classified as harmful oxygenates [19, 20, 21]. By contrast, high yields of phenolic compounds and furans are desired as they increase the economic value of the bio-oil. Higher content of phenolic compounds and furan are preferred for the production of aromatic hydrocarbons which lead to better suitability for the fuel production [19, 22]. The bio-oil composition can be modified into designated ingredients by employing for example a higher catalyst-to-feed ratio [23].

Table 2 Model Component of Bio-oil for Simulation [6, 10]

Functional Group	*Model Component*	
	VTT	*NREL/PNNL*
Organic acid	Acetic acid	Crotonic acid
Alcohols	Ethyleneglycol,acetol	1,4-benzenediol $C_6H_6O_2$
Aldehydes	Glycol aldehyde	3-methoxy-4-hydroxybenzaldehyde
Sugar derivatives	levoglucosan	levoglucosan
Ketones	-	hydroxyacetone
Furans	furfural	furfural
Extractives	oleic acid	dehydroabietic acid
Sulfur	ethylthioethanol	Dibenzothiophene
nitrogen	2-pyrrolidone	2,4,6-trimethylpyridine
Phenolics/ lignin	guaiacol (LMLa) pyrolignin (HMLa)	isoeugenol, cellobiose, dimethoxystilbene, dibenzofuran, oligomeric compounds with a β-O-4 bond, phenylcoumaran compounds

Due to the complexity and vast amount of constituents, modelling bio-oil for simulation become challenging. Therefore, several institutions develop a model to simplify lists of bio-oil compounds inputted into simulation [6, 10]. The model, displayed in Table 2, represents each category of bio-oil ingredients by selecting one or two major component. Such modelling step significantly enhance the convergence of the simulation with negligible errors [10].

2.1.2 Screw Reactor

Currently, most pyrolysis practices are fast pyrolysis conducted in fluidized bed due to its superiority in providing the highest liquid yield. Moreover, fluidized bed offered effective heat transfer and suitable to large-scale plant. Nonetheless, the reactor also possesses several

drawbacks such as dilution of pyrolysis vapor. Such dilution lower the concentration of pyrolysis vapor which leads to a difficulty in product separation [10]. Hence, various pyrolyzer types, including screw reactor, are developed as an improvement measure. Table 3 compared the performance of fluidized bed and screw reactor.

Table 3 Comparison between Screw Reactor and Fluidized Bed [24, 25]

	Screw Reactor	Fluidized bed
Advantages	- More flexible to particle size without significantly changing the process parameters - Smaller reactor offers lower capital investment	- Uniform temperature - More favorable to higher scale
Disadvantages	- Poor heat transfer causes temperature gradient - Prone to mechanical wear	- Larger volumes of inert carrier gasses diluted the pyrolysis vapor - The presence of char and ash poisoned catalyst and reduced the capability of catalyst - More complex and consume more energy due to sand recirculation system

Contrast to the fluidized bed, the screw reactor eliminates the need of large volume of inert carrier gas thus reduces the risk of pyrolysis vapor dilution [24] and lowers the energy loss to the heat carrier. Additionally, recent studies also mention that the type of pyrolysis reactor along with the reaction condition contribute to bio-oil composition [7, 24].

2.2 Vapor Upgrading

Vapor upgrading purposes mainly to eliminate oxygenates from the bio-oil, either via catalytic upgrading or hydrotreatment. Catalytic upgrading pathways are superior in various factors, such as (1) required no hydrogen supply, (2) operated at atmospheric pressure thus suppressed costs and (3) produce aromatic compound which possesses a potentially higher market value as fuel additives and chemical feedstock [1]. Catalytic upgrading is commonly catalyzed by (H)ZSM-5. Studies by Diebold et al. and Dutta et al. observed that during vapor upgrading process, oxygen removed by three distinct mechanisms: (1) decarbonylation by ejecting CO, (2) decarboxylation by ejecting CO_2 and (3) hydrodeoxygenation by ejecting H_2O [8, 26]. Another study by Yildiz et al. also discovered a similar consequence of upgrading process: the yield of bio-oil decreased whereas water and gas content increase [23]. Even though several research have revealed the mechanism of upgrading, the net heat involved in the bio-oil upgrading reaction is scarcely discussed. Jeczmionek et al. investigated the net heat of those three reactions [27] in fatty acid in vegetable oil instead of oxygenates in bio-oil. They detected that both hydrodeoxygenation and decarboxylation of fatty acid are exothermic while decarbonylation is slightly endothermic [27].

2.2.1 Comparison between Ex-situ and In-situ Upgrading

The upgrading process of pyrolysis vapor can be executed directly after pyrolysis process in the same reactor or off-line in another reactor. The direct process is called in-situ or catalytic fast pyrolysis (CFP) whereas the off-line is ex-situ. Currently, CFP model is more widely operated. The similar configuration to fluid catalytic cracking (FCC) system in conventional petroleum refinery promotes the adaptability of CFP to existing process [28]. Moreover, CFP utilizes single reactor for both pyrolysis and upgrading process instead of two separated reactor,

as shown in Figure 2. As a result, CFP costs lower investment for the new installation. Nonetheless, ex-situ configuration outperformed CFP concerning catalyst deactivation [6]. In addition, ex-situ upgrading also offers advantages in optimizing each process [29]. As pyrolysis and upgrading process is conducted in a separated reactor, each of them can be operated at its optimum temperature. The temperature of the catalyst in upgrading process defined carbon selectivity of olefins and aromatics [13]. Therefore, ex-situ provided better controllability and flexibility [13].

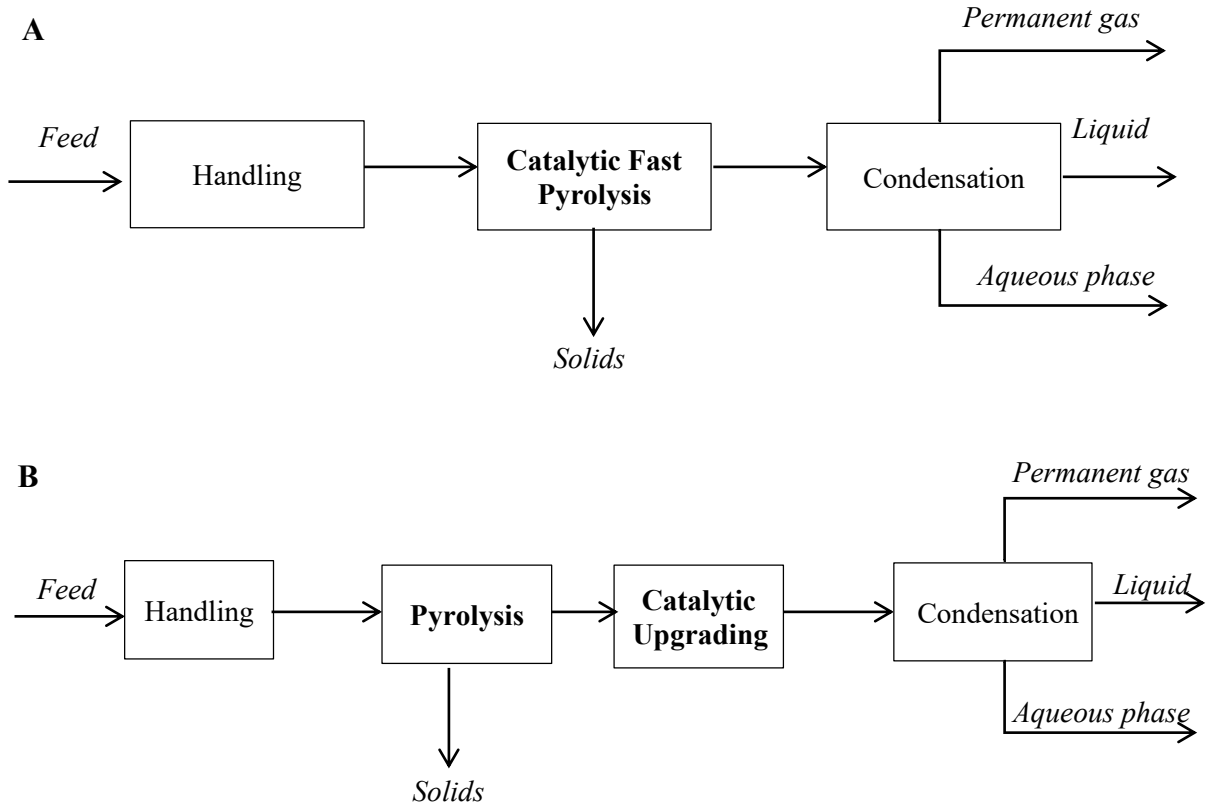

Figure 2 Process block flow diagram of in-situ (a) and ex-situ (b) upgrading

Coke formation is observed as one of the crucial problems in vapor upgrading. Previous studies mentioned coke formed via two major pathways: polymerization and dehydration-condensation [29, 30]**.** In the dehydration-condensation reaction, the primary pyrolysis vapor contained various unstable larger molecular which more active to form carbon deposits on catalyst surface [13]. Whereas in polymerization mechanism, the aromatics compound polymerized to form coke. The catalyst deactivation phenomenon is significantly faster in in-situ configuration. Detail comparison between in-situ and ex-situ configuration is summarized in Table 4.

Table 4 Comparison between in-situ and ex-situ upgrading [6]

	In-situ	Ex-situ
Costs	Lower capital cost; higher operating cost	Higher capital cost as separated reactor needed but lower operational cost
Catalyst deactivation	Severe irreversible deactivation rate because of contact with inorganic matter	Lower catalyst deactivation due to the less contact with of ash or inorganic matter
Operating condition	Closely tied to fast pyrolysis	Flexibility to be operated at different conditions than the pyrolysis. As a result, ex-situ possessed higher carbon efficiency and lower deactivation rate
Solids separation	Catalyst mixed with solids and biomass	Char (including the ash) separated prior to upgrading, reducing the risk of ash poisoning to the catalyst
System option	Limited to fluidized bed	Fluidized bed or fixed bed. A fixed bed can be employed for precious metal catalysts. For feasibility reason, the coke formation required to be reduced

2.2.2 Comparison between Fixed Bed and Fluidized Bed

As formerly mentioned, ex-situ offers flexibility in upgrading vapor either in a fixed bed or fluidized bed. Table 5 compared the advantages and disadvantages of each reactor. Even though the fluidized bed is a popular reactor for biomass pyrolysis and upgrading [13], fixed bed configuration prevents undesired fluid catalyst attrition. It is more flexible to catalyst type especially precious metal, thus providing better control over chemistry reaction and product composition [8]. Fixed bed system is potentially cost higher investment but lower catalyst cost which lead to comparable total cost [8].

Table 5 Advantages of fixed bed and fluidized bed as ex-situ upgrading reactor [8, 31]

Fixed bed	Fluidized bed
- lower rates of particle attrition - flexible to precious catalysts - suitable for lower scale systems	- continuous and quick catalyst regeneration - low pressure-drop - ability to add and withdraw particles without interrupting the operation

2.3 Pretreatment and Separation Process

Similar to pyrolysis and vapor upgrading process, feedstock pretreatment and product separation process are also played a crucial role. Appropriately complying parameters listed in Table 6 are essential to achieve desirable product and process.

Table 6 Key Parameters in Designing Vapor Upgrading [32]

Process	Crucial Parameters
Pretreatment	Feed is essential to dry into 10% wt. of MC or less, commonly utilizes low-grade heat. Small size particle required.
Pyrolysis	Wood conductivity limits the heat transfer The optimum temperature for liquid production is 500ºC
Solids Separation	Most of ashes and inorganic compounds retained in char. Poor solids separation can result in: - secondary cracking of the vapor phase catalyzed by mineral contents of char - acceleration of the slow polymerization which manifested in increasing viscosity
Vapor Upgrading	Oxygen content preferably below 25% wt. of oil
Product Collection	- Bio-oil product optimized via rapid cooling of the vapor. - Time and temperature profile between vapor formation and quenching affects the composition and quality of bio-oil. Prolong the exposure of high temperature continues vapor cracking. - Fuel-designated bio-oil tolerate vapor residence time up to 2 s - Blockage of differential condensation of heavy ends can be avoided by careful design and temperature control.

2.3.1 Pretreatment

Prior to pyrolysis process, commonly biomass is subjected to two pretreatment processes: drying and comminution. Drying is essential as water caused adverse properties to bio-oil whereas commonly biomass received in high moisture, i.e. 20%-30% wt. moisture. Completely dry biomass subjected to drying still contains about 10% wt. water. However, further drying of biomass can lead to the loss of volatile organic content (VOC) and the risk of fire. Commonly, drying executed by contacting biomass with low humidity air in elevated temperature [33]. One technology that applied this method is belt dryer. Belt dryer operates at low temperature with input gas flow at 90ºC -110ºC and exhaust at 60ºC-70ºC [33] to prevent the emission of VOC [34].

The second important step is comminution as it enhances the heat transfer within the biomass. As mentioned in Table 6, heat conductivity of biomass limits the heat transfer. Accordingly, a smaller particle size helps to adequately exploit heat transfer [35]. Further, particle size along with the residence time will significantly affect bio-oil composition [36, 37]

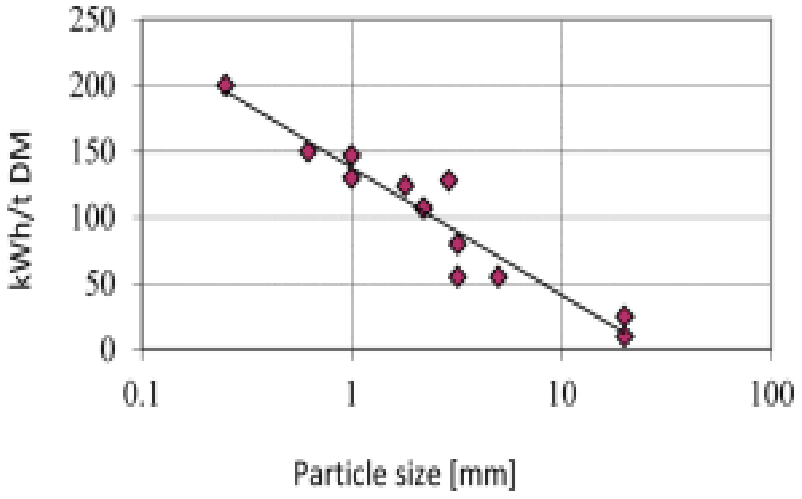

Figure 3 Energy consumption for grinding of wood [10]

Furthermore, char developed at the surface during pyrolysis also possess insulating properties. Figure 3 presented that the energy consumed by grinding process is in inverse proportion to particle size.

2.3.2 Solids Separation

Rapid separation of char and ash from pyrolysis gas is highly preferable to prevent secondary cracking. The inorganic content in ash and char can act as a catalyst and lead to further thermal cracking [8]. Thus, the pyrolysis gas ought to be filtered to separate gas from solids such as fine char and ash. Solid-gas separators can be classified into two broad groups based on their separation methods: external forces and barriers [38]. Two common examples of the external forces group are cyclone and electrostatic precipitator (ESP) while examples of barriers method are bag filter.

Table 7 contrasted each type of filters. Due to its simplicity and low price, a cyclones is considered as the first choice for general particulate separation. However, it poorly separates fine particles which emitted by almost all pyrolysis [8]. For this reason, in actual practices cyclone tandem with either ESP or bag filter.

Table 7 Comparison of Gas-Solid Separator [39, 40]

Device	Capture Mechanism [40]	Efficiency (%) [39]	Cost (USD) [39]	
			Capital (in 1982)	Operational (per ton removal*)
Cyclone	Inertial concentration	87	10500	1.68
ESP	Particle charging and migration to plates	98.3	96500	2.84
Bag filter	Cake formation	99.9	49000	3.14

**price at 10MW thermal*

2.4 Current Experiments in Ex-situ Catalytic Upgrade

Recently, studies of pyrolysis in a screw reactor tandem with ex-situ catalytic upgrading in a fixed-bed reactor have been developed in pilot scales. Bosong et al. and Li et al. installed their system in similar configuration [24, 16] as depicted in Figure 4. Bosong et al. aimed to investigate the effect of temperature into product distribution by varying pyrolysis temperature within range of 400-600ºC in single catalyst type, i.e. HZSM-5. On the other side, Li et al. examined the significance of various zeolites catalyst type by conducting pyrolysis at 500ºC.

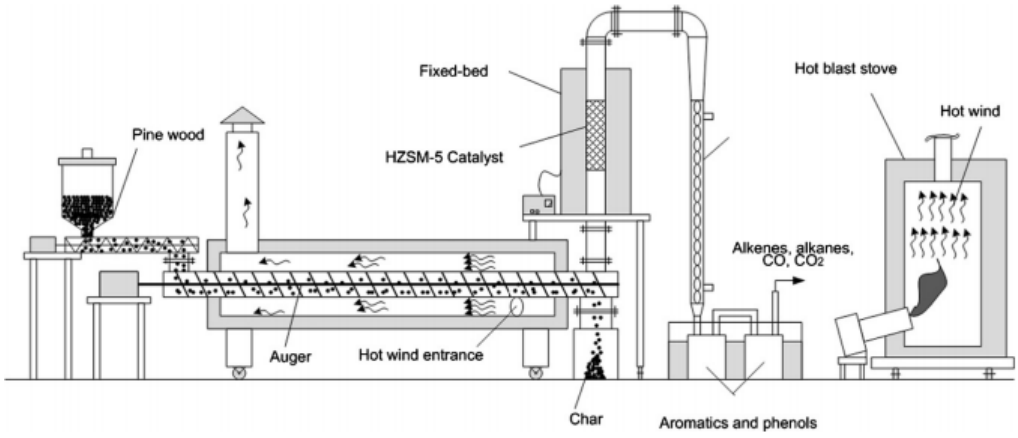

Figure 4 Configuration of ex-situ catalytic upgrading screw pyrolyzer integrated with fixed bed [24, 16]

Both studies carried out slow pyrolysis processes. The heat consumption of pyrolysis reactor is provided by combustion of non-condensable gas along with diesel. By the end of screw reactor, char is collected while pyro-gas is directly sent for upgrading without any filtration. The fixed bed upgrading reactor packed with catalyst and operated at a temperature range of 450-650ºC. Subsequent to catalytic upgrading process, the vapor is condensed in a water-cooling condenser followed by two traps in series immersed in chilled water.

Similar to study by Li et al., Guda et al. separately performed a study on the effect of catalyst type. However, the operating condition is slightly different. Guda et al. pyrolyzed pine wood at 450ºC [17]. Contrast to Li et al., Guda et al. performed the upgrading at a lower temperature than pyrolysis i.e. 425ºC. These three experiments, mainly their configuration, are then considered in developing simulation in this report.

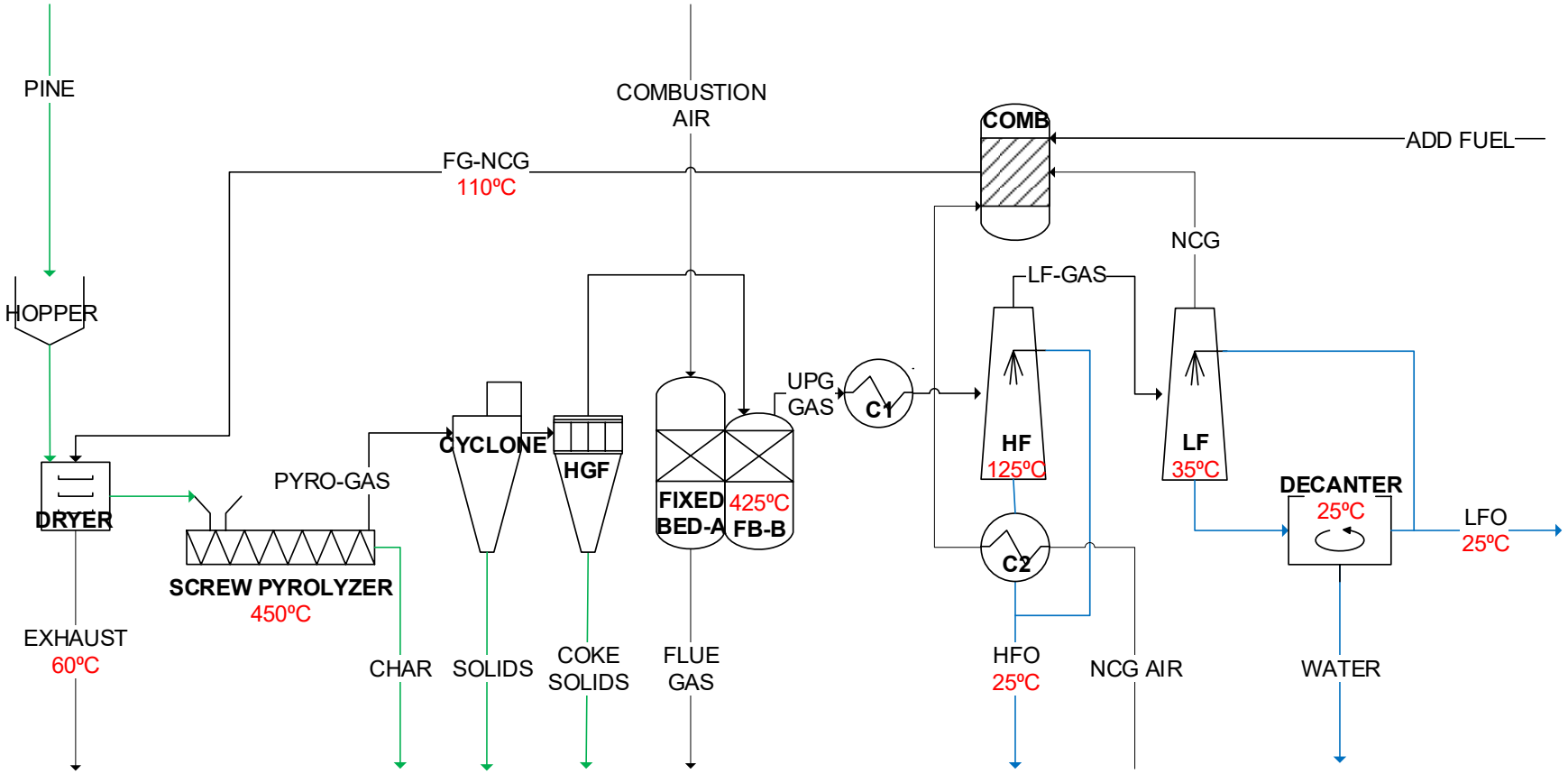

Figure 5 the layout of the overall process

3 METHODOLOGY

This section aims to describe the layout of the process as well as the procedures in developing the simulation model. The section covers four vital topics: (1) process overview, (2) procedures for collecting data, (3) the development of simulation and (4) calculations. The boundary conditions of the simulation model are also addressed at the end of this chapter.

3.1 Process Overview

The main systems for pyrolysis and ex-situ catalytic upgrading is built based on six sections [32, 6, 41]. They are (1) feedstock handling and preparation, (2) pyrolysis section, (3) vapor filtration, (4) catalytic vapor upgrading section and catalyst regeneration, (5) vapor quenching and condensation and (6) the non-condensable gas (NCG) combustion. The whole process layout is available in Figure 5.

3.1.1 Feedstock Handling and Preparation

The handling and preparation of the biomass section aims to treat the pinewood so it fits for the pyrolysis reaction regarding moisture content and particle size. In this simulation, the grinding step is eliminated as the screw reactor is more flexible to large feed particle compare to fluidized bed reactor [7, 16]. As a consequence, the sawdust particle size is assumed within the acceptable particle size for screw reactor. Figure 6 shows that the pinewood is dried by blowing flue gas from NCG combustion. As a reference case, the wet biomass is assume to possess moisture content of 50%wt. and dried into 8%wt. [10] Due to economic reasons, belt conveyor dryers are selected for biomass drying. Flue gases are supplied at 110ºC and exhausted at 60ºC following the common practice of belt-dryer [33].

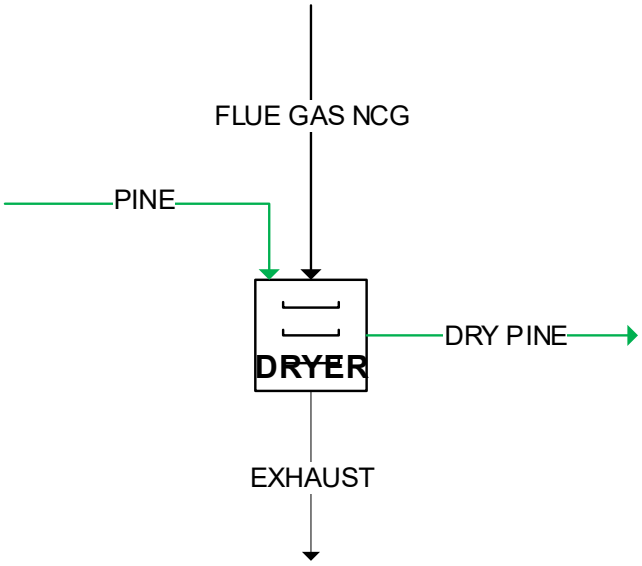

Figure 6 Feedstock Handling and Preparation

3.1.2 Pyrolysis

The pyrolysis process conducted in screw reactor at 450ºC [42] heated by electricity and heat loss of the reactor assumed to be 10%. The decision of the usage of electric heater instead of other option is based on the economical reason [43]. The screw reactor is operated continuously without the presence of carrier gas or heat carrier [42]. Even though the pyrolysis essentially produced aerosols [42], aerosols are assumed absence in product lists [10] as depicted in Figure

7 to simplify the simulation. The char is collected as a product while pyro-gas is processed in the next phase. Due to the relatively low temperature of pyrolysis, most of the mineral content of pinewood is sequestered in the char [35].

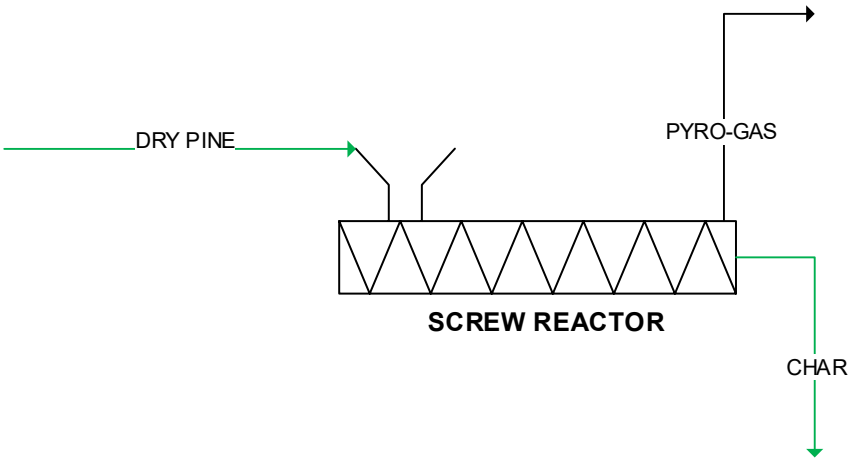

Figure 7 Pyrolysis in Screw Reactor

3.1.3 Vapor Filtration

The pyrolysis is continued by vapor filtration. The vapor is separated from char and solids particle in the cyclone and hot gas filter, presented in Figure 8, prior upgrading. The filtration process is necessary to eliminate ash content in vapor as well to avoid fouling of the catalyst bed which cause catalyst deactivation. A quick and effective separation process is significant as char can catalyze a further vapor cracking and contribute to the production of polyaromatic hydrocarbons [44].

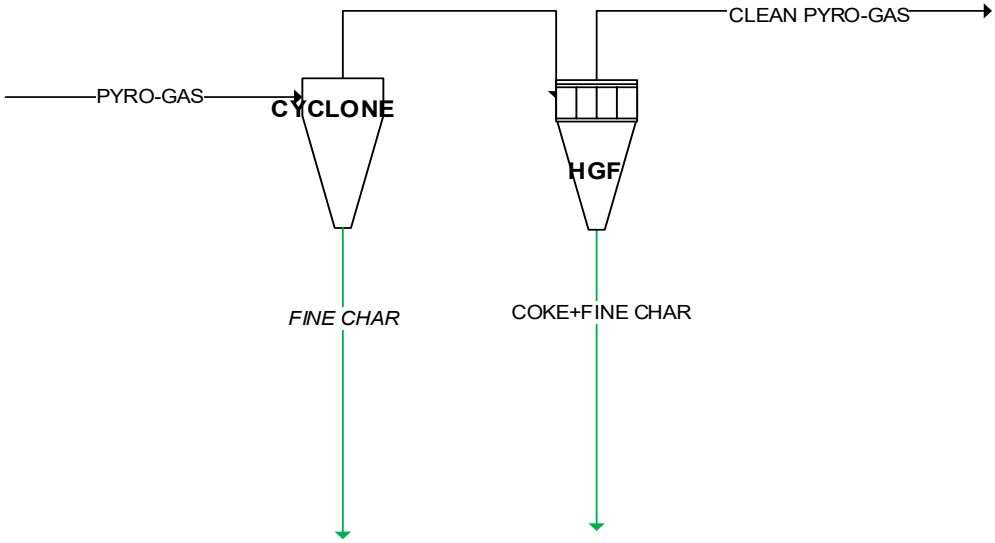

Figure 8 Vapor Filtration

Larger solid particles are removed by the cyclone while fine particles are eliminated in the hot gas filter (HGF) with the type of ceramic candle filter. Nevertheless, HGF increased carbon losses via additional solids and light gases formation during filtration process [8]. The carbon loss is assumed to be 10%wt. of the feed carbon content, relying on the range of losses reported [8]. Coke formation is assumed to be endothermic reflecting on pyrolysis reaction which is also expected to be endothermic. Thus, HGF operates at a lower temperature (425ºC) than cyclone

(450ºC). To accommodate the wide variation of cyclone efficiency, i.e. 70–90% [45], cyclone assumed to perform 80% efficiency. Remaining 20% solids are eliminated in HGF.

3.1.4 Vapor Upgrading and Catalyst Regeneration

The flow of pyrolytic vapors with a lower content of particulate matter is then upgraded in a catalytic fixed bed reactor at 425ºC to reduce the oxygen content. Such upgrading temperature is adopted from existing study [17]. Heat loss assumption is 5%. The process catalyzed by HZSM-5 and online catalyst weight is 5% of the feedstock [17]. The upgrade process, visualized in Figure 9, generated a mixture of gas which contains NCG, water vapor and organics.

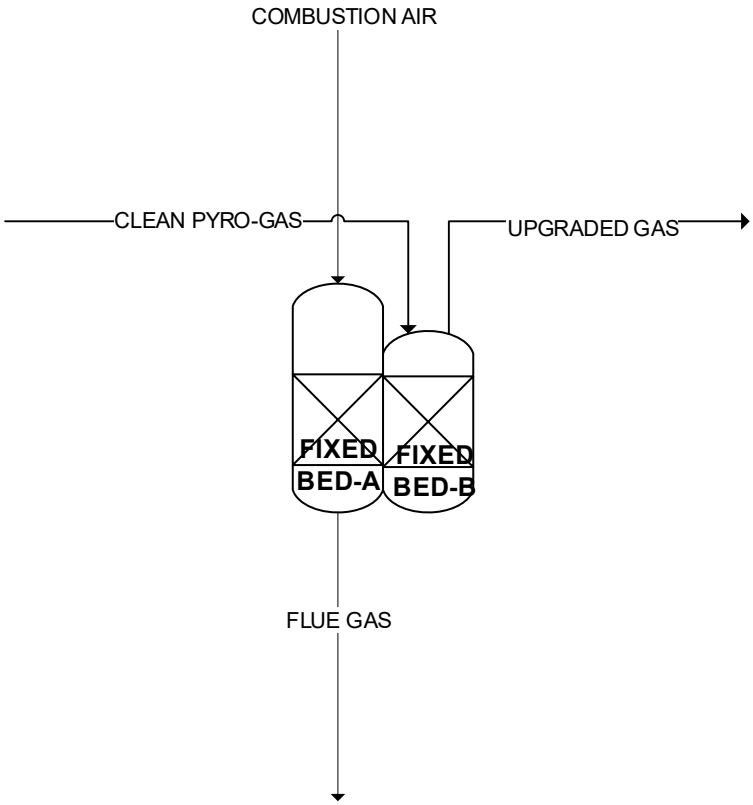

Figure 9 Ex-situ Upgrading in Fixed Bed Reactor

Additionally, coke is also formed during the upgrading process as a result of cracking. The accumulation of coke covered the active site of catalyst and deactivated them. Thus, the catalyst is regenerated by burning the spent catalyst. Regeneration implemented at 700ºC [8] to avoid catalyst deterioration. Subsequently, the flue gas is cooled into its dew point before being released to the atmosphere. Since the catalyst periodically regenerated, two fixed bed reactor are installed in parallel. During the regeneration process of reactor A, the upgrading is conducted in the backup fixed bed reactor i.e. reactor B. As a character of ex-situ upgrading, the combustion heat of coke is unrecovered [6].

3.1.5 Vapor Quenching and Condensation

Upgrading process is continued by quenching to rapidly condense vapor into bio-oil. Prior to the quenching process, upgraded gases are cooled into proximately its dew point to minimize the amount of oil recycling. In most experiments, both heavy fraction bio-oil (HFO) and light

fraction bio-oil (LFO) are solely cooled by LFO [6]. However, in this report, each vapor is quenched by corresponding recycled bio-oil to enhance the condensation of HFO. The quenching system consisted of two scrubbers in series and a decanter unit as shown in Figure 10. The first scrubber, HF, separated the HFO from light gases. The second scrubber, LF, separated the LFO including water from NCG. As the moisture content of the light fraction oil is more than 30% wt. [24], it underwent a phase separation [10]. Thus, LFO required further separation with water in a decanter which operated at 25ºC. Whereas decanter operating temperature can easily be decided solely according to the ambient temperature, determining the operating temperature of scrubbers required further investigation. The determination of operating temperature of LF and HF should consider bio-oil compositions. Otherwise, bio-oil poorly separated and the process excessively recirculated oil for quenching. All measures and results related to this consideration are elaborated in chapter 4. By the end of condensation, both heavy and light oil is cooled into 25ºC prior to avoid aging. The heat released by oil cooling is partially recovered to preheat the air for NCG combustion.

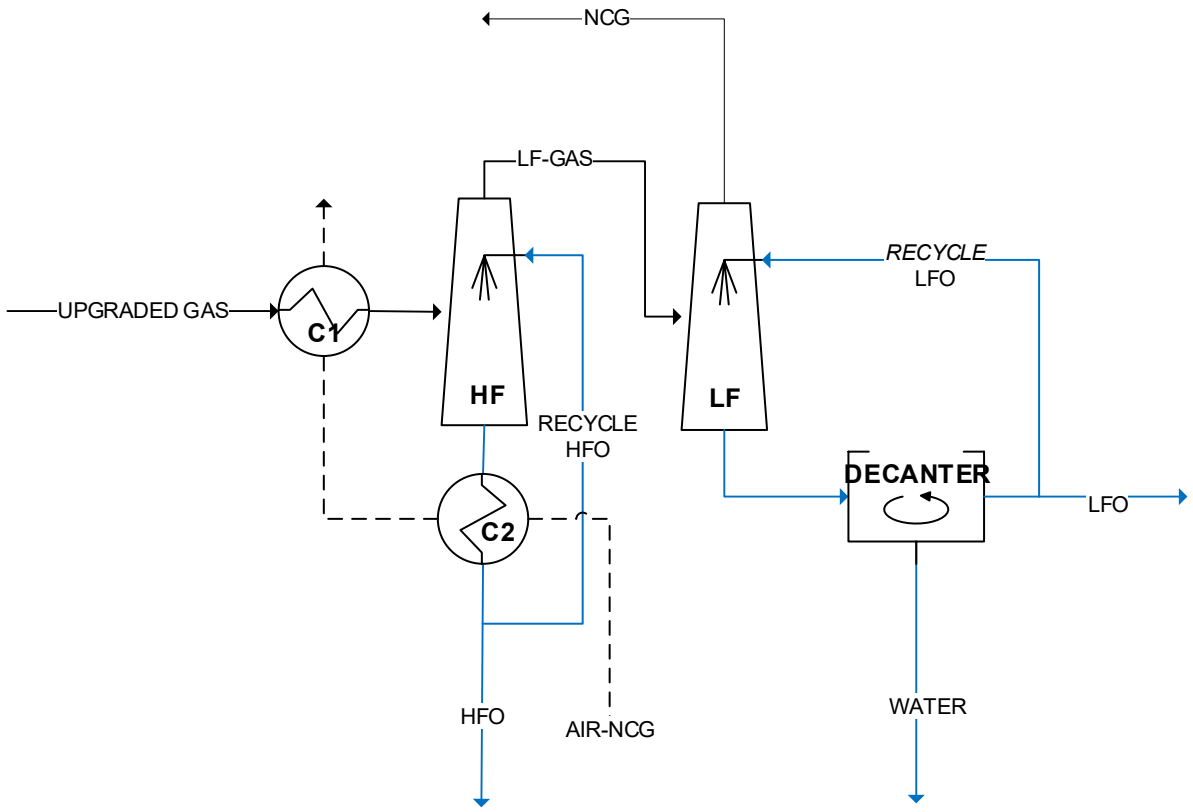

Figure 10 Vapor Quenching and Condensation

3.1.6 Non-condensable Gas Combustion

NCG discharged from LF scrubber is combusted to cover the heat for feedstock drying. Excessive combustion air along with extra fuel is added, if necessary, to maintain flue gas of the combustion at 110ºC and supplied at the adequate amount for the drying process. Prior to combustion, the air is preheated by recovering heat from HFO cooling process extracted in C1 and C2. However, the heat from LFO cooling is unrecovered due to low temperature.

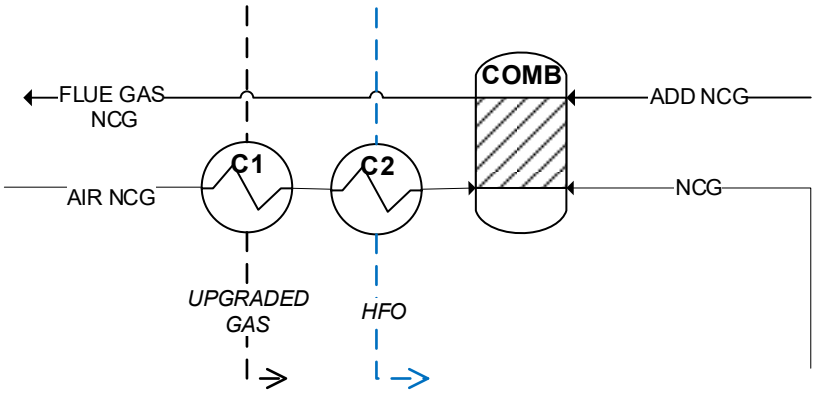

Figure 11 NCG combustion

3.2 Data Collection

Pyrolysis in screw reactor with ex-situ catalytic upgrading is a newly developed process. The integration of screw pyrolyzer with fixed bed catalytic reactor for ex-situ catalytic upgrading has been scarcely studied [17]**.** As a consequence, data for the simulation are barely available. The simulation is mainly based on results of two separated experiments conducted by Ingram et al. and Guda et al. Ingram et al. examined pyrolysis of debarked loblolly pine in an auger reactor at 450ºC with no upgrading process [42]. In 2016 Guda and Toghiani improved Ingram's experiment by adding ex-situ upgrading process in a fixed bed reactor at 425ºC [17]. These two experiment results are chosen as main sources considering that both authors had conducted pyrolysis using the same reactor and the same feedstock. All missing information are then gathered from various related sources. Section 3.2 aims to encapsulate all essential data for the simulation.

3.2.1 The Analysis Data of Feedstock

Feedstock for the system is debarked loblolly pinewood sawdust with feed-rate 80 kg/hour. Table 8 lists the pinewood composition. The ultimate analysis are adjusted from the original data by converting dry ash free basis into dry basis.

Table 8 Ultimate and Proximate Analysis of debarked Loblolly Pinewood [46]

Ultimate Analysis (% wt.)	
Carbon	47.42
Hydrogen	4.97
Oxygen	46.93
Nitrogen	0.10
Ash content	0.58

Proximate Analysis (%wt.)	
Ash content	0.58
Moisture content	50.00
Volatile matter	86.20
Fixed carbon	13.20

3.2.2 Yield of Products

Table 9 exhibits the original data as well as the final adjusted data for simulation input for pyrolysis and vapor upgrading processes. Unlike yield for ex-situ upgrading, the original data for pyrolysis yield results are displayed in range form. Thus, the exact value for pyrolysis simulation are then determined by considering accessible supporting data. Nonetheless, product yields of upgrading process are also prescribed adjustment since coke formation is omitted which violated the actual phenomenon.

The char yield of pyrolysis is presumed to be equal to the char yield defined by Guda et al. Char yield is expected to be independent of the catalytic reaction as it produced in screw reactor [17]. The reaction condition of the pyrolysis process which utilized no solids as heat carriers and poor heat transfer suggested that the reaction classified as slow pyrolysis. Instead, the yield of char provided by Ingram et al. i.e. 17% wt., is within the range of char yield of fast pyrolysis [10, 12] and significantly lower than typical slow pyrolysis which approximately 30%wt. [11, 12]. For this reason, heat and mass balance in pyrolyzer possibly subjected to inaccuracy.

Table 9 Product Yield of Pyrolysis and Upgrading of Loblolly Pinewood [17, 42]

	Original Data		***Data for Simulation***	
	Pyrolysis[a]	*Ex-situ Upgrading[b]*	*Pyrolysis[a]*	*Ex-situ Upgrading[b]*
Temperature [ºC]	450	425		
Product yields (%wt.)				
Char	17.5-19.8	17	17[b]	17[b]
Gas (NCG)	33.8-25.0	49	33.8	43.6
Bio-oil	48.7-55.2	34	49.2	30.3
moisture content	*16*	*7.37*	*16*	*37.0*
Coke				
Hot gas filter	-	-	-	*1.25*
Fixed bed catalyst				*7.87*

Other three yields i.e. gas, bio-oil and coke, are calculated based on mass conservation. Mass balance, equation 1, is the basic governing equation in defining product yield. For the pyrolysis process, equation expanded into elemental balance 2-5, for each process component to calculate the product. Detail steps on each calculation described in the section 3.2.3 until 3.2.6.

$$\dot{m}_{inlet\ stream} = \dot{m}_{outlet\ stream} \quad (1)$$

$$C_{pinewood} = C_{bio-oil\ (dry)} + C_{char} + C_{NCG} \quad (2)$$

$$H_{pinewood} = H_{bio-oil(dry)} + H_{char} + H_{NCG} + H_{water} \quad (3)$$

$$O_{pinewood} = O_{bio-oil(dry)} + O_{char} + O_{NCG} + O_{water} \quad (4)$$

$$N_{pinewood} = N_{bio-oil\ (dry)} + N_{char} \quad (5)$$

$$1 = X_{bio-oil(dry)} + X_{char} + X_{NCG} + X_{water} \quad (6)$$

3.2.3 The Yield of Non-condensable Gas (NCG)

Compositions of NCG for both pyrolysis and upgrading process are given by the experiment results of Bosong et al. as presented in Table 10 [24]. Such measure applied considering the similar operating condition: decreasing temperature of pyrolysis to upgrading. Bosong et al. conducted an experiment of pinewood pyrolysis in auger reactor at 500ºC followed by ex-situ upgrade process in fixed bed reactor at 450ºC. In addition to elemental balances, the calculation of NCG yield also considered the higher heating value (HHV) of resulted char. Gopakumar et al. mentioned pyrolysis in such condition produced char with HHV, calculated using equation 7, within range of 26-27 MJ/kg db [47].

Table 10 Non-condensable gas composition [24]

Components	*NCG pyrolysis*		*NCG catalytic upgrade*	
	(%vol)	*(%wt)*	*(%vol)*	*%wt*
CH_4	6.17	2.86	6.17	2.86
C_2+alkane	0.83	0.67	0.83	0.67
C_2+alkene	1.26	0.95	1.26	0.95
C_6H_6	0.11	0.25	0.11	0.25
CO_2	46.74	59.66	46.74	59.66
CO	43.75	35.54	43.75	35.54
H_2	1.14	0.07	1.14	0.07
HHV (MJ/kg)				6.22

$$HHV = 33.8\, m_C + 144.2 \left(m_H - \frac{m_O}{7.94}\right) \left[\frac{MJ}{kg\ dry}\right] \quad 7$$

Because changes in NCG yield affected HHV of char, NCG yield is varied from 25%wt. to 33.8%wt. [17] to obtain char possessing such HHV value. As a result, 33.8%wt. of NCG provided char with HHV equal to 23.5 MJ/kg-dry. On the other hand, the yield of NCG after the upgrading process is adjusted from the original data by including the amount of coke, explained in section 3.2.6. Its final yield is equal to 43.6%wt.

3.2.4 The Yield of Bio-oil

As yields of char and NCG are already derived, the yield of bio-oil is the difference of their sum, as formulated in equation 6. Bio-oil yielded 49.2% wt. The water content of 16%wt. of oil is directly copied from Ingram et al. [42]. Similar to the yield of NCG for upgraded process, the yield of bio-oil produced from the ex-situ upgrade are also adjusted, mainly related to coke formation and water content. The water content in bio-oil subsequent to ex-situ upgrade process is evaluated since the initial value mentioned by Guda et al., 7.37% wt., is considered too low. Alternatively, NREL assumed the water content of bio-oil is 11% wt. of the dry feed [8] or equal to 37% wt. of bio-oil. Moreover, such assumption is supported by a statement that water content of bio-oil after upgrading process is commonly higher than 30% wt. of oil [10].

3.2.5 The Composition of Bio-oil

The elemental composition of bio-oil in Table 11 are directly extracted from two primary sources [17, 42]. Contrast to the original source, the elemental composition of bio-oil inputted into simulation are regarded as water-free composition. Otherwise, it violated the HHV range of char [47] within NCG yield limits, see section 3.2.3. Such elemental data infer as the initial data to further adjust the detailed chemical composition of the bio-oil.

Table 11 Elemental components of bio-oil [17]

Elements	*Raw Pyrolysis oil (% wt.)*	*Upgraded bio-oil (% wt.)*
C	52.64	69.40
H	7.53	7.23
N	0.09	0.23
O	39.52	23.14

Chemical composition of bio-oil of pyrolysis and upgraded oil are based on two aforementioned main sources. However, they are significantly modified to satisfy the elemental balance of bio-oil. Both sources represent the bio-oil composition by listing approximately 30 chemical compounds. Essentially, it is impossible to completely identify the content of bio-oil [10]. Therefore, accessible compounds are primarily assumed to represent the whole composition of bio-oil. In order to simplify and enhance the convergence during the Aspen Plus simulation, component lists are grouped into nine major function groups following model described in Table 2.

The experiment result by Ingram et al. are modified by considering experiment result by Gopakumar et al. to maintain the elemental balance of pyrolysis oil. Table 12 displayed those two result subsequent to classification. Note Gopakumar et al. stated the concentration of furfural are similar to guaiacol and 1,2-benzenediol is considerably less [47].

Table 12 The classified composition of pyrolysis oil from two different experiments

Components	*Classified composition of pyrolysis oil (% wt.)*	
	Ingram et al. [42]	*Gopakumar* [47]
Acetol	4.79	6
Furfural	2.53	16
Dextrose	51.99	53
1,2-benzenediol	25.70	5
Guaiacol	11.73	16
Benzoic acid	0.33	3
Vanilin	1.49	
Oleic acid	1.45	

In the other hand, Ingram et al. mentioned that furfural is dramatically less while the amount of 1,2-benzenediol are more than twice of guaiacol [42]. Considering these contradictions, values of those three components are iterated and adjusted. Final result concluded in Table 14.

The upgraded bio-oil is modified from Guda data due to lack information of unit for the aromatic component. Guda et al. mentioned the oxygenate components of upgraded bio-oil in mass concentration units, i.e. µg/mL methanol, while the aromatic components are only stated in percentage of GC area as summarized in Table 13. The analysis method of Ingram et al. that 2 grams of bio-oil is diluted per mL of methanol are assumed applicable to experiments by Guda et al. Thus, such information gave the conversion factor of µg/mL methanol to percent weight of bio-oil. By assuming all oxygen content in upgraded oil is originated from oxygenates, the percent weight of aromatics can be derived. Final composition of upgraded oil presented in Table 14.

Table 13 Initial upgraded bio-oil composition subjected to classification [17]

Components	*Amount*	*Unit*
Acetol	392.50	µg/mL
Furfural	439.10	µg/mL
Dextrose	73.56	µg/mL
1,2-benzenediol	3272.58	µg/mL
Guaiacol	3263.46	µg/mL
o-xylene	9.39	%GC area
1,2,3-trimethylbenzene	5.02	%GC area
2,6-dimethylnaphtalene	7.49	%GC area
Indene	2.13	%GC area

Table 14 Final compositions of pyrolysis oil and upgraded oil

Components	*Pyrolysis oil (% wt.)*	*Upgraded oil (% wt.)*
Acetol	4.12	4.27
Furfural	12.36	4.78
Dextrose	51.99	0.80
1,2-benzenediol	16.53	35.62
Guaiacol	11.73	35.52
Benzoic acid	0.33	
Vanilin	1.49	
Oleic acid	1.45	
o-xylene		7.43
1,2,3-trimethylbenzene		3.97
2,6-dimethylnaphtalene		5.93
Indene		1.69

3.2.6 The Yield of Coke

Although coke formation is a significant aspect in the mass and energy balance of the catalytic fixed bed reactor, the exact amount of coke formation is unknown. In a separate study, NREL explained that coke forms in two parts of the system: hot gas filter as well as catalytic reactor [6, 8]. Guda et al. mentioned that the amount of coke formation in the catalyst is approximately 26% of catalyst weight [17]. Assuming catalyst loading rate of 5% wt. of dry feedstock [17] resulted in coke formation 1.25% wt. of feedstock due to upgrading. The second source of coke formation is HGF. NREL mentioned 10% wt. of carbon of the feedstock loss as coke in HGF [8]. Coke is expected to be composed by carbon, hydrogen, and oxygen, detail result explained in Table 15. Given all these information, an additional iteration step is required to determine the total mass of coke formed while maintaining the elemental balance. All equations involved in the calculation is described further in section 3.2.6. The calculation resulted in coke formation of approximately 7.87%wt. of the dry pinewood.

3.2.7 Elemental Composition of Char and Coke

The elemental composition of char and coke derived by calculating the difference among elemental composition of pinewood, bio-oil, and non-condensable gas. The mass conservation

law presented in equation 1 are transformed into three elemental balance, equations 8-10. The elemental composition of char and coke are easily defined since yields of all products are already derived. The final char and coke composition is summarized in Table 15.

$$[C_{bio-oil} + C_{NCG}]_{screw} = \left[C_{bio-oil} + C_{coke} + C_{non-condensable\ gas}\right]_{fixed\ bed} \quad 8$$

$$[H_{bio-oil} + H_{NCG} + H_{water}]_{screw} = [H_{bio-oil} + H_{coke} + H_{NCG} + H_{water}]_{fixed\ bed} \quad 9$$

$$[O_{bio-oil} + O_{NCG} + O_{water}]_{screw} = [O_{bio-oil} + O_{coke} + O_{NCG} + O_{water}]_{fixed\ bed} \quad 10$$

$$1 = \left[X_{bio-oil(dry)} + X_{coke} + X_{NCG} + X_{water}\right]_{fixed\ bed} + X_{char} \quad 11$$

Table 15 Elemental component of biochar and coke (by-difference)

Elements	*Char (% wt.)*	*Coke (% wt.)*
C	58.50	55.71
H	6.63	13.86
N	0.32	0.41
O	31.92	30.03
Ash	2.63	
HHV dry (MJ/kg)	23.5	32.02

3.3 Aspen Plus Model

A steady-state Aspen Plus simulation model is developed to examine the mass and energy balance of the overall system. The model involved four non-conventional solids, namely biomass, char, coke and ash. Non-conventional solids defines as a non-pure chemical species which properties are absent in Aspen Plus databank. Instead, Aspen Plus calculates their enthalpy and density according to component composition provided by the user. In this model, enthalpies and density of non-conventional components are calculated by COALGEN and COALIGT respectively. Ultimate and proximate analysis inputted into simulation are based on data in section 3.2. Therefore, model streams are specified as MIXNC due to the presence of non-conventional solids. Further, most of the process simulation applied equation of state Peng-Robinson with Boston-Mathias modifications (PR-BM) to accommodate non-ideality of the system [6]. Previous studies commonly use either UNIQUAC or Peng-Robinson model [6, 8, 10]. As a reference case, the received pinewood sawdust is assumed to contain 50% wt. moisture [10].

3.3.1 Feedstock Drying

A drying process is essential to yield dry sawdust with 8% wt. moisture content. The drying process is simulated by two prime blocks and two manipulators. Two primary blocks are stoichiometric reactor (RStoic) and flash separator (Flash2) as shown in Figure 12 . RStoic is preferred to represent the removal of water from the wet pinewood even though drying involved no chemical reaction. The process within the dryer is represented by reaction $Pine \rightarrow 0{,}0555804\ H_2O$. By default, Aspen Plus defines the molecular weight of a nonconventional compound is equal to 1 g/mole [48]. Thus, number 0.0555804 represents the mole of water formed in each mass loss from pine. Since the temperature of drying is considered low, the process is assumed to be adiabatic. Thus the heat duty of Rstoic is set to 0.

Streams	*Description*
PINE	Wet pine
FG-NCG1	Flue gas of NCG combustion
EXHAUST	Moist flue gas stream
D-PINE	Pine with 8%wt. moisture

Blocks	*Description*
DRYER	Part of the dryer where water evaporation occurred
DRY-SEP	Outlet part of the dryer

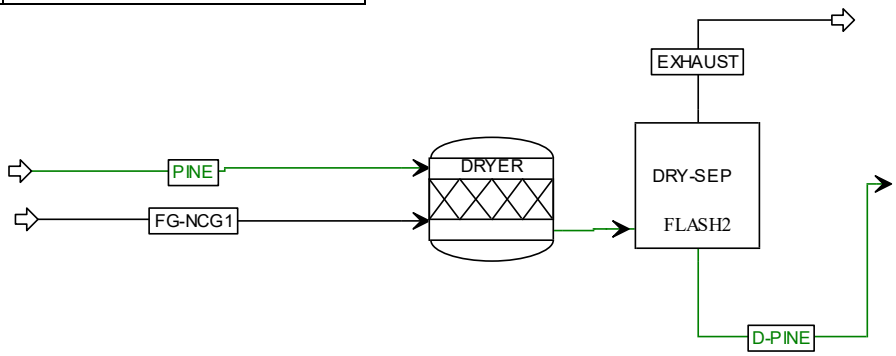

Figure 12 the model of feedstock drying process

Two manipulators involved are calculator and Design Spec. A calculator block is added to control drying to simplify any changes in moisture of dry pine stream. Similarly, Design Spec block is added to manipulate the mass flow of FG-NCG1 by setting EXHAUST temperature at 60ºC.

3.3.2 Pyrolysis

The screw reactor is simulated by RYield continued by SEP to model the separation of char from the pyro-gas by the end of the reactor as displayed in Figure 13. RYield is selected since the product distribution is available instead of the kinetics and stoichiometric of reactions. The 10% heat loss of pyrolysis process simulated by a multiplier block named M-SCREW and a Design Spec block. Design Spec manipulated the amount of S-IN heat stream thus stream S-OUT equal to 0.

Streams	*Description*
D-PINE	Pine with 8%wt. moisture
CHAR	Particle char
PY-GAS	Pyrolysis gas
S-IN	Heat input of screw reactor
S-OUT	Heat output of screw reactor

Blocks	*Description*
M-SCREW	Manipulator of heat loss of screw reactor
SCREW-R	Screw reactor
SEP	Outlet of screw reactor

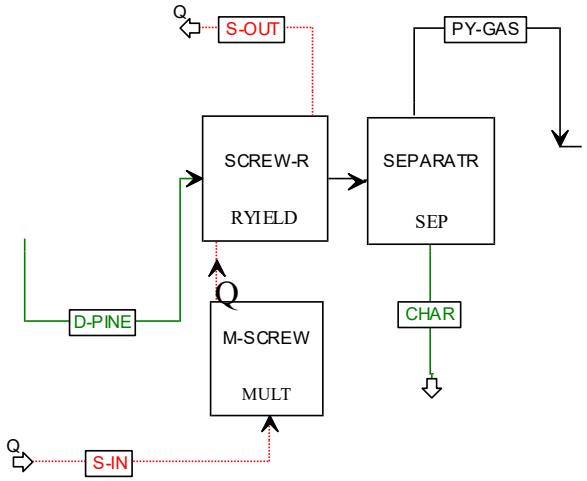

Figure 13 the model of the pyrolysis process

3.3.3 Vapor Filtration

Pyro-gas is filtered by a cyclone and a hot gas filter as mentioned in section 3.1.3. Figure 14 described the cyclone is modelled by SSplit block while the hot gas filter (HGF) is essentially simulated by Flash2 block.

Streams	*Description*
PY-GAS	Pyrolysis gas
PY-GAS1	Clean pyrolysis gas outlet of the cyclone
PY-GAS2	Clean pyrolysis gas outlet of HGF
MIX	Pyrolysis gas and coke-ash mixture
ASH	Fine char discharged from the cyclone
COKE1	Coke formed in HGF
D-IN	Heat input of DEC block
D-OUT	Heat output of DEC block

Blocks	*Description*
CYCLONE	Cyclone
HGF	Hot gas filter
DEC	Part of HGF where coke is formed
M-DEC	Manipulator of heat loss of DEC

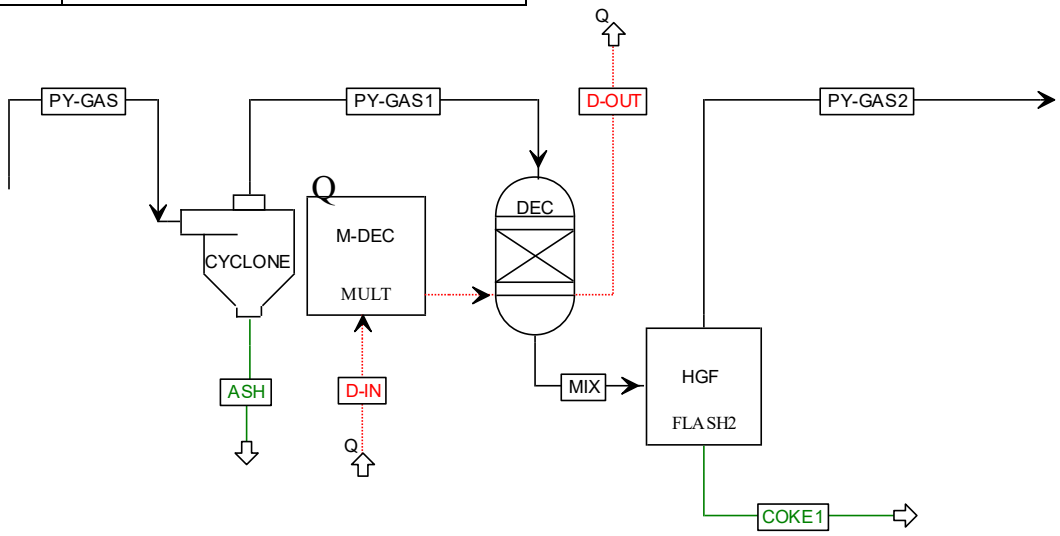

Figure 14 the model of vapor filtration process

The split fraction of ash in cyclone is defined 80% of total ash. RYield block identified as DEC is also added to simulate the decomposition of pyro-gas partially into coke. Likewise in

pyrolysis simulation, the 5% heat loss is characterized by multiplier block. Both DEC and HGF blocks operated at lower temperature i.e. 425ºC even though cyclone functioned in 450ºC. Assumed as such since coke formation is expected to be endothermic.

3.3.4 Vapor Upgrading and Catalyst Regeneration

The vapor upgrading system is simulated by RYield block, a multiplier and a Flash2 block as limned in Figure 15. RYield is selected due to similar reason to pyrolysis process. Multiplier represented 5% heat loss. During upgrading process, coke is formed and covered catalyst. Thus, Flash2 block is present to imitate the actual separation of coke covering catalyst and the upgraded vapor within the reactor. The spent catalyst regenerated in a system visualized in Figure 16.

Streams	*Description*
PY-GAS2	Clean pyrolysis gas outlet of HGF
UPG-GAS	Upgraded gas with coke
UPG-G1	Clean upgraded gas
COKE2	Coke covering catalyst
FB-OUT	Heat output of fixed bed reactor

Blocks	*Description*
FIX-B	Fixed bed reactor
M-FB	Manipulator of heat loss of fixed bed
FB-SEP	Outlet part of fixed bed reactor

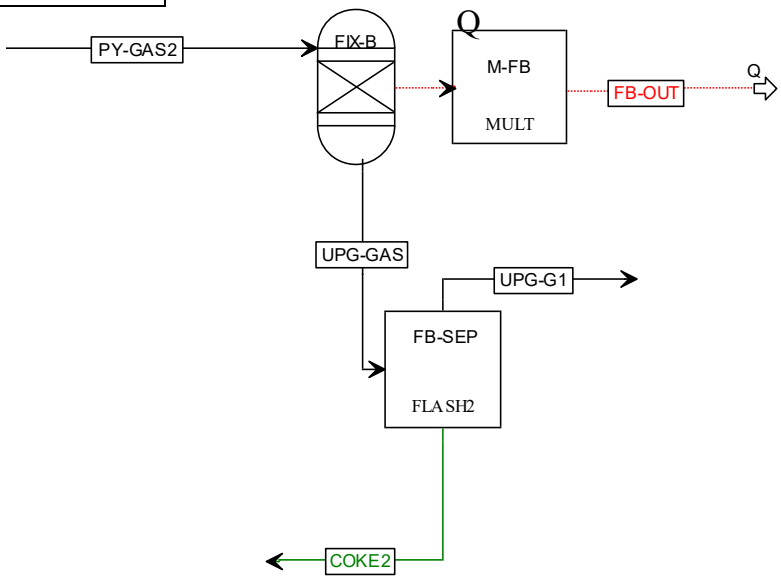

Figure 15 The model of vapor upgrading process

Generally, coke combustion process is simply simulated by Gibbs reactor. All possible products (H_2O, CO_2, C, H_2, N_2 and O_2) are specified as mixed sub-stream except C which is specified as a 'PureSolid' sub-stream. However, Figure 16 depicted Gibbs reactor (REG) preceded by RYield (C-DEC). Since non-conventional components in Aspen Plus including coke uninvolved in a chemical reaction, it necessitated to be decomposed into its constituents prior to combustion. The heat absorbed during decomposition process is supplied from the combustion process. The combustion temperature is controlled by a Design Spec block by varying combustion air. Finally, the flue gas is then cooled into 25ºC before discharged into the atmosphere.

Streams	*Description*
COKE2	Coke covering catalyst
AIR-C	Air for catalyst regeneration
FG	Flue gas of coke combustion
C-FG	Cold flue gas
Q	Heat of coke decomposition

Blocks	*Description*
C-DEC	Coke decomposition part of regenerated fixed bed reactor
REG	Regenerated fixed bed reactor

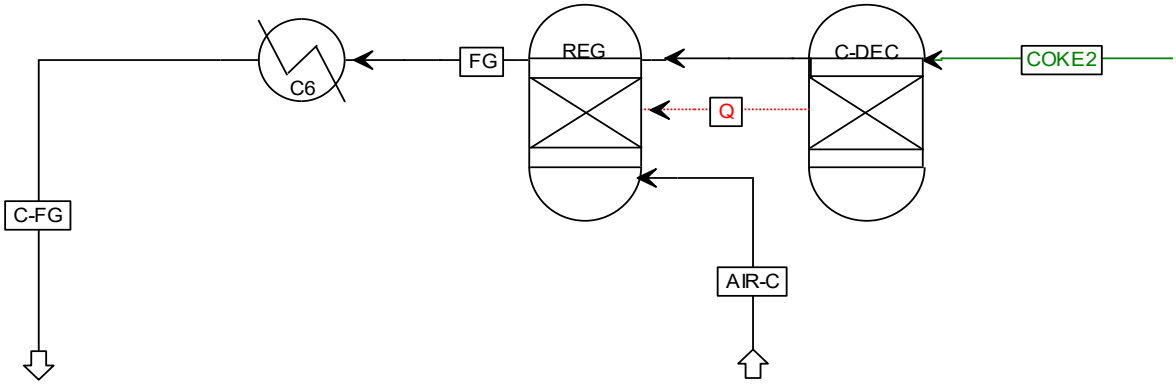

Figure 16 the model of catalyst regeneration process

3.3.5 Vapor Quenching

The vapor quenching system is modelled by two Flash2 blocks, HF and LF, and a decanter as visualized in Figure 17. Flash2 block is considered to sufficiently represent single stage condensation and phase separation [49]. Prior to quenching the upgraded gas UPG-G1 is cooled to 170ºC, just above its dew point, to minimize the demand for oil recycling. HF and LF are operated at different temperature to optimize separation and minimize oil recycle. HF is operated in varying temperature, between the dew point of HFO and LFO, to acquire the optimum temperature. Similar reason to HF, LF is also operated between 25ºC until the dew point of water vapor. Further, LFO is separated from water in DECANT block. Since moisture content in LFO exceeded 30%wt., it presented two-phase liquid [10]. Hence, the valid phase for LF and DECANT blocks are set into Vapor-Liquid-Free Water to accommodate the presence of water in the condensate.

Regarding oil recirculation, a stream loop is avoided in the simulation to prevent error during simulation. Instead, Transfer and Design-Spec blocks are employed to mimic looping process. Two transfer blocks copied compositions of each oil, REC-HFO1 to REC-HFO and REC-LFO1 to REC-LFO respectively. Finally, mass-flow of REC-LFO and REC-HFO are manipulated by Design-Spec to achieve operating temperature of scrubbers.

Streams	*Description*
UPG-G1	Clean upgraded gas
REC-HFO	Recirculated HFO
REC-HFO	Dummy recirculated HFO
LF-GAS	Light fraction upgraded gas
HFO-C	Cold HFO
REC-LFO	Recirculated LFO
REC-LFO	Dummy recirculated LFO
NCG	Non-condensable gas
LFO	Light Fraction Gas
WATER	Condensate water
LFO-C	Cold LFO

Blocks	*Description*
HF	Quenching tower for clean upgraded gas
C1	UPG-G1 cooler
C2	HFO cooler
LF	Quenching tower for light fraction upgraded gas
DECANT	Decanter

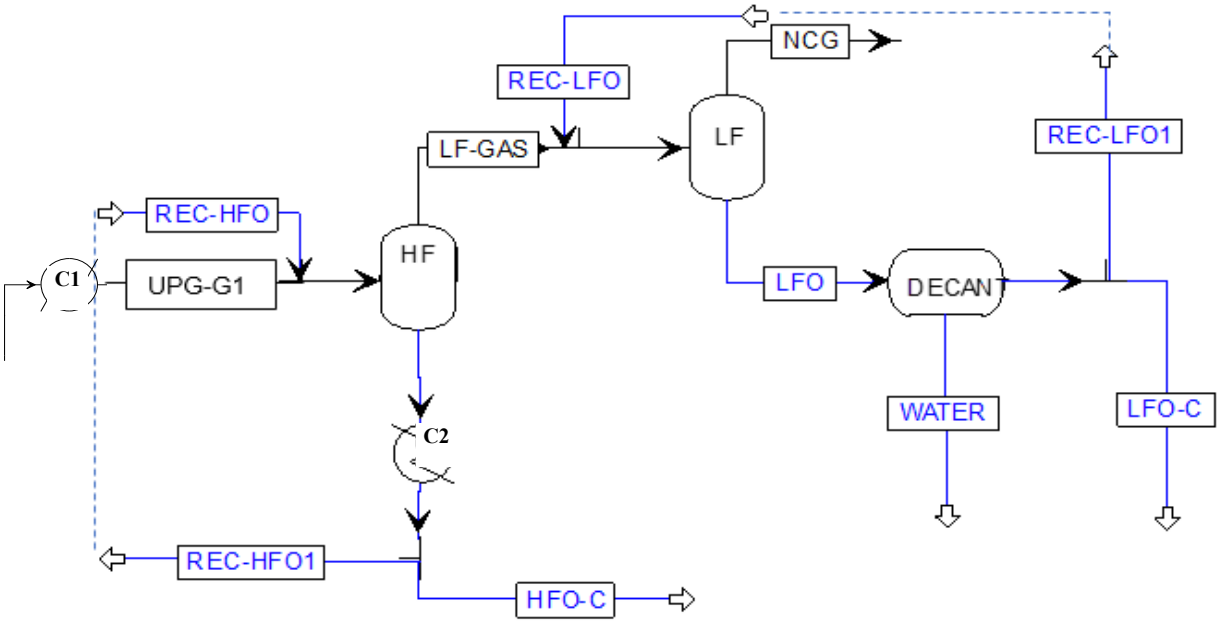

Figure 17 the model of vapor quenching process

3.3.6 Non-condensable Gas Combustion

The combustion of NCG is modelled by RGibbs block. All setting in RGibbs are similar to those in coke combustion system. Prior to combustion, the combustion air is preheated by heat recovered from the cooling process. Its flow is manipulated by Design-Spec to fulfill the requirement of drying process mentioned in section 3.3.1. As depicted in Figure 18, an extra line for natural gas is installed to maintain the temperature of the flue gas FG-NCG at precisely 110ºC.

Streams	*Description*
C-AIR	Air for NCG combustion
NCG	Non-condensable gas
ADD-NG	Added fuel (natural gas)
FG-NCG	Flue gas from NCG combustion

Blocks	*Description*
HX	Air preheater using oil heat recovery
COMB	Combustor

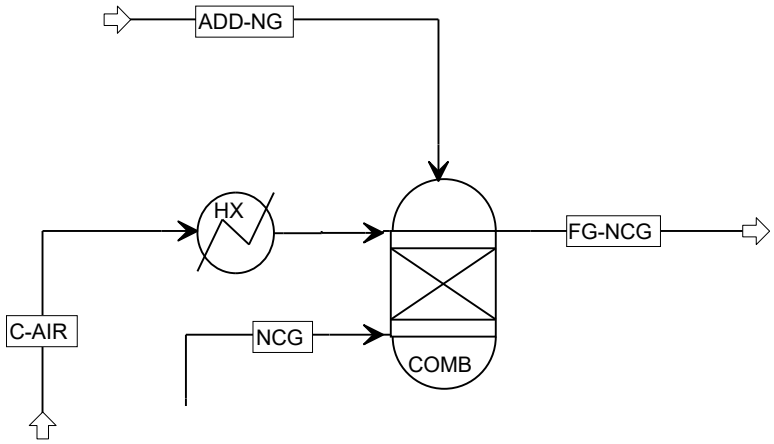

Figure 18 the model of NCG combustion process

3.4 Calculations

In addition to Aspen Plus simulation, the energy balance of each reactor involving solids and bio-oil are also manually calculated to fully understand the principal work of the software as well as to investigate if results from both method are similar. As previously mentioned, solids properties in Aspen Plus are estimated by particular procedure called COALGEN while enthalpy of bio-oil is specified by selecting 8-9 major components as representatives. Contrast to Aspen Plus, enthalpy of solids are manually calculated by combining HHV calculated by Dulong's formula and heat capacity from empirical formula. While enthalpy of bio-oil are estimated by applying empirical formula.

There are five unit process involves solids and bio-oil. They are drying, pyrolysis, vapor filtration, vapor upgrading, and vapor quenching. However, manual calculation excludes the energy balance of vapor quenching due to difficulties in forecasting heat of vaporization for bio-oil [11]. Therefore, this step only executes four unit process: drying, pyrolysis, vapor filtration, and catalytic upgrading. In general, calculations can be divided into two categories: (1) heat balance without reaction and (2) heat of reaction. The first category observed in the drying process while the second category covered pyrolysis, filter and fixed bed. Furthermore, calculations also assessed mass and energy efficiencies as well as the economic aspect of the overall system.

3.4.1 Heat of Drying Process

In the drying process, sensible heat released by the flue gases are consumed to partially evaporate water and increase the temperature of the wood as formulated in equation 12. The heat of evaporation and sensible heat of wood defined by formula 15 and 13 respectively. Latent heat of water is calculate further by equation 16, taken from Perry et al. [50]. On the other hand, the heat capacity of wood involved in equation 13 is defined based on empirical formula 14 by Yang et al. [11]. At 60ºC the latent heat of water is 2363.5 kJ/kg while the wood heat capacity is 1.25 kJ/kg.K.

$$Q_{drying} = Q_{sensible\ wood\ (8\%\ wt.\ MC)} + Q_{water} \quad 12$$

$$Q_{sensible} = \dot{m} \times Cp \times \Delta T \quad 13$$

$$Cp_{dry\ wood}\ (T) = 3.50\ T - 89.68\ \left[\frac{J}{kg.K}\right] \quad 14$$

$$Q_{water} = \dot{m} \times (H_{vaporization} + Cp_{water\ vapor} \times \Delta T) \quad 15$$

$$H_{vap} = 5.2053\ (1 - T_r)^{0.3199 - 0.212T_r + 0.25795{T_r}^2}\ \left[\frac{J}{kmol}\right];\ T_r = \frac{T\ [K]}{T_c\ [K]} \quad 16$$

3.4.2 Heat of Reaction

The general concept of energy conservation to calculate the heat of reaction is captured in equation 17. Standard enthalpy of formation and heat capacity of all involving components are unavailable except for NCG; thus, they obliged further calculation. The standard enthalpy formation for char and pine are calculated by equation 18. HHV associated to such equation are calculated by Dulong's equation, previously stated in equation 7. While heat capacity of char and pine is given by equation 23 and 14 respectively.

Enthalpy of bio-oil is calculated by equation 19-22. Dry bio-oil properties are calculated by empirical formulas from a study by Yang et al. [11]. Note that bio-oil is considered in its vapor phase since the pyrolysis temperature is high enough to prevent the condensation of bio-oil. All constants involved in determining the heat of formation (equation 19) and sensible heat (equation 22) of bio-oil listed in Table 16.

$$Q_{reaction} = \sum n_{out}(H_f^\circ + \Delta H)_{out} - \sum n_{in}(H_f^\circ + \Delta H)_{in} \quad 17$$

$$HHV_{solids} = \sum n_{flue\ gas\ out}(H_f^\circ)_{flue\ gas\ out} - \sum n_{solids}(H_f^\circ)_{solids} \quad 18$$

$$H_{f_k}^\circ = a + b_1\frac{H}{C} + b_2\left(\frac{H}{C}\right)^2 + b_3\left(\frac{H}{C}\right)^3 + b_4\left(\frac{H}{C}\right)^4 + c_1\frac{O}{C} + c_2\left(\frac{O}{C}\right)^2 + c_3\left(\frac{O}{C}\right)^3 + c_4\left(\frac{O}{C}\right)^4\ \left[\frac{kJ}{kmolC}\right] \quad 19$$

$$H_k(T) = H_{f_k}^\circ + \int_{298.15}^{T} Cp_k\ (T)\ dT \quad 20$$

$$\Delta H_k(T) = R_{\Delta H,k} \int_{298.15}^{T} Cp_{methane}\ (T)\ dT \quad 21$$

$$R_{\Delta H,k} = d + e_1\frac{H}{C} + e_2\left(\frac{H}{C}\right)^2 + e_3\left(\frac{H}{C}\right)^3 + e_4\left(\frac{H}{C}\right)^4 + f_1\frac{O}{C} + f_2\left(\frac{O}{C}\right)^2 + f_3\left(\frac{O}{C}\right)^3 + f_4\left(\frac{O}{C}\right)^4 \quad 22$$

$$Cp_{char,coke}\ (T) = 3.23\ T - 100.01\ \left[\frac{J}{kg.K}\right] \quad 23$$

The calculation for heat reaction of process elaborated from the general heat balance into a detailed formula 24-26. Note equation 25 only involved bio-oil and coke because each mass of coke formed in the filter is assumed as the product of bio-oil decomposition.

$$Q_{pyro} = H_{char}(T_{out}) + H_{bio-oil}(T_{out}) + H_{gas}(T_{out}) - H_{pine}(T_{in}). \quad 24$$

$$Q_{coking} = H_{coke}(T_{out}) + H_{bio-oil}(T_{out}) - H_{bio-oil}(T_{in}) \quad 25$$

$$Q_{upgrading} = H_{coke}(T_{out}) + H_{bio-oil}(T_{out}) + H_{NCG}(T_{out}) - H_{bio-oil}(T_{in}) - H_{NCG}(T_{in}) \quad 26$$

Table 16 Constant for calculating enthalpy formation and $R_{\Delta H,k}$ [11]

Constant of H_f°	Value	*Constant of* $R_{\Delta H,k}$	Value
a	11.725	*d*	0.358
b_1	41.864	e_1	0.096
b_2	-57.075	e_2	0.066
b_3	17.739	e_3	-0.014
b_4	-1.639	e_4	$0.4993 \cdot 10^{-3}$
c_1	-166.770	f_1	0.477
c_2	20.594	f_2	-0.883
c_3	-64.368	f_3	0.936
c_4	25.368	f_4	-0.269

3.4.3 Efficiency

The mass and energy efficiency of bio-oil calculated by equation 27-28. If the screw reactor is electrically heated, the energy input for pyrolysis multiplied by 2.5 to accommodate the conversion of thermal heat into electricity during electricity generation. The conversion efficiency is assumed to be 40%.

$$\eta_{oil,mass} = \frac{\dot{m}_{bio-oil}}{\dot{m}_{dry\ pine}} \quad (27)$$

$$\eta_{oil,energy} = \frac{Q_{bio-oil}}{Q_{pine}+Q_{drying}+Q_{pyrolysis}+Q_{coking}} \quad (28)$$

3.4.4 Economic Aspect

A simple economic aspect is addressed by calculating the profit of bio-oil and char production per mass of pinewood. All price involved are listed in Table 17. The plant is assumed to consume a moderate amount of electricity, thus categorized as 1C industry in Swedish Energy Agency classification. While in income calculation, bio-oil is assumed to have density similar density to water, 1 kg/L.

Table 17 Assumption of Average Price Involving in Profit Calculation

Variable		Unit Price		Ref
Cost	Pinewood sawdust	0.787	SEK/kg-dry	[9]
	Electricity	0.188	SEK/MJ	[43]
Income	Char	4	SEK/kg	
	Bio-oil	7	SEK/kg	

3.5 Boundary Account

The investigated system consists of the drying process, screw pyrolyzer combined with fixed catalytic bed, then followed by vapor quenching process. The study excluded the simulation and analysis of flue gas cleaning, ash handling, and the treatment of aqueous phase of the plant.

4 RESULTS AND DISCUSSION

The section covers four vital topics: (1) energy and mass balances of each unit process, (2) bio-oil mass and energy efficiency, (3) economic analysis and (4) comparison with existing upgrading technology. All energy balances present in this section are based on HHV.

4.1 Energy and Mass Balance

Four unit processes i.e. drying, pyrolysis, HGF, and vapor upgrading are modelled using both Aspen Plus and spreadsheet tool in Microsoft Excel. The essential difference between those methods is the calculation of bio-oil properties. Whereas spreadsheet tool employed empirical formulas, bio-oil in Aspen Plus is represented by 8-9 compounds thus its properties derived based on the combined properties of each component. Overall, results of energy balance from the manual calculation are insignificantly differed from those from Aspen Plus simulation, as enlisted in Table 18. Pyrolysis unit yields the maximum gap i.e. 8.5% error while another two processes, coke formation and catalytic upgrading, exhibited similar gaps.

Table 18 shows that the energy balance calculated from Aspen Plus simulation are consistently lower than results from the manual calculation. Besides different steps in determining bio-oil properties, such differences are expected inherited from properties of solids. Properties of solid compounds such as biomass, char, and coke are unavailable in Aspen Plus databank. Thus, their HHV are calculated by COALGEN method as described in section 3.3. Essentially, COALGEN calculated HHV of solids in the same route as manual calculation, i.e. equation 18 section 3.4 [51] but they refer to different databanks. As a result, HHV calculated by Aspen Plus are constantly *ca*. 3% higher than those from manual method.

Table 18 Comparison between simulation and manual calculation results

Process	*Ideal heat of reaction (MJ)*		*Difference*
	Simulation results	*Manual Calculation*	
Drying	93.0	92.3	0.7%
Pyrolysis	53.24	58.21	8.5%
Coke formation HGF	8.06	8.35	3.5%
Catalytic Upgrading	-2.09	-2.01	3.9%

In additional to HHV gaps, different results are also caused by heat capacity. Substantial temperature different in pyrolysis between the inlet (60ºC) and outlet temperature (450ºC), which absent in other processes, lead pyrolysis to possess the highest result difference. Note heat capacity applied in the manual calculation is estimated by empirical formula taken from Yang et al. [11]. Energy balance for pyrolysis from manual calculation is considered to be more precise than simulation. Therefore, energy and mass balance of pyrolysis unit refers to manual calculation results while other units refer to Aspen Plus simulation. Detail explanation of each unit process described in section 4.1.1 until 4.1.6.

4.1.1 Feedstock Drying

The feedstock is dried in a belt conveyor by flowing flue gas of NCG combustion at 110ºC. Due to belt conveyor restriction, the drying gas is exhausted at 60ºC [33]. Figure 19 exhibited that the process demands almost 2 tons of flue gas to dry 80 kg/h feedstock from 50%wt. moisture content into 8%wt. moisture content. The direct contact during drying transfers 36.52

kg of water from wet biomass to the gas thus increases moisture content of the drying gas from 0.26%vol. to 3.1%vol. Table 19 summarizes detail compositions of gases before and after drying.

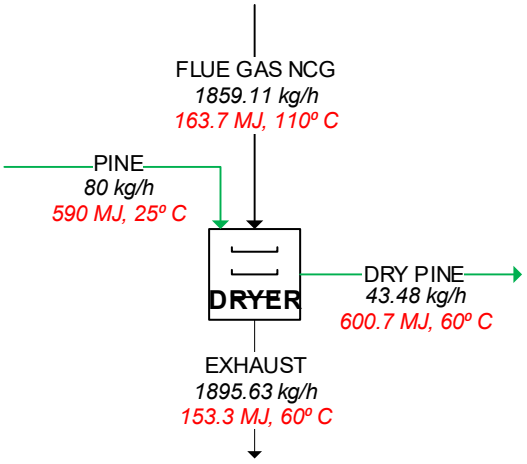

Figure 19 Mass and Energy (based on HHV) Balance in Feedstock Dryer

Essentially, flue gas NCG preferred to be cooled into its lowest possible temperature to exploit whole energy available without exceeding its dew point and violating pinch point rule. The water content in exhaust gas with moisture content 3.37% vol. condensates at 27ºC. Whereas assuming biomass supplied at 25ºC and temperature different for pinch point is 10ºC led to the lowest exhaust temperature of flue gas of 35ºC. In short, flue gas is potentially able to be cooled into 35ºC. Such measure reduces the amount of flue gas NCG to 1173 kg/h. Thus, the actual amount of gas demand is 58% wt. higher than the theoretical amount needed in ideal condition. This value reflects belt conveyor characteristic i.e. to offer 46-58% efficiency [33].

Table 19 Components of flue gas NCG before and after drying

Parameters	*Flue gas NCG*	*Exhaust*
Temperature	110ºC	60ºC
Components (%vol.)		
H_2O	0.26	3.37
CO_2	0.90	0.96
O_2	19.74	19.64
N_2	79.10	76.03

Since drying consume a vast amount of energy and less efficient, the process provide opportunity for improvement. One alternative for improvement is to re-combust the exhaust in NCG combustion, considering its high oxygen content. This option is discussed further in section 4.1.6. The change of moisture content also significantly affected the energy consumption of the system. Effects of moisture is further discussed in section 4.2.

4.1.2 Pyrolysis

As expected, Figure 20 visualized that pyrolysis is an endothermic reaction. The ideal heat absorbed for pyrolysis by neglecting heat loss is 1.46 MJ/kg dry biomass or equal to 9.87% HHV of dry pinewood. This result is comparable to the result reported by Hua Yang et al. which also investigated the pyrolysis of pine in screw reactor [11]. Hua Yang et al. reported

that pyrolysis at 600ºC consume 1.5 MJ/kg dry biomass and lower number is expected for lower pyrolysis temperature [11]. In general, the heat of reaction for slow and fast pyrolysis found in literature is tabulated in Table 20 and compared with the results obtained in this study.

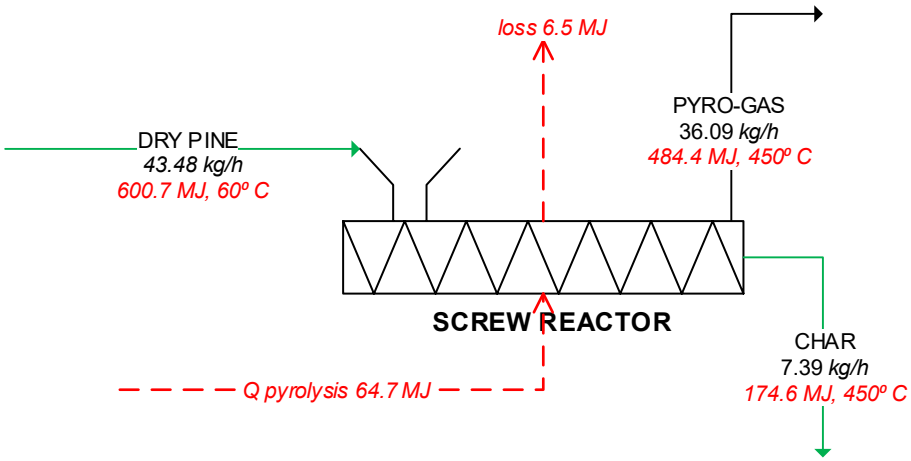

Figure 20 Mass and Energy (based on HHV) Balance in Screw Reactor

The energy requirement for fast pyrolysis is 18% higher in a twin screw mixing and 30% higher in a fluidized bed. As previously mentioned in section 0, one of the drawbacks of fast pyrolysis is energy loss due to heat carrier [24]. Fast pyrolysis consumed extra energy to heat solids as heat transfer medium into reaction temperature. The consumption of additional energy is even more amplified in a fluidized bed as it also heated the fluidizing gas.

Table 20 Comparison of pyrolysis heat between slow and fast pyrolysis

Operation condition		*Q pyrolysis (MJ/kg dry feed)*	*Difference (%)*	*Ref*
Slow pyrolysis	450ºC, screw reactor	1.46	0	
	600ºC, screw reactor	1.5	2.6	[11]
Fast pyrolysis	480ºC, fluidized bed	1.9	30.0	[10]
	500ºC, twin screw mixing	1.77	18	[52]

4.1.3 Vapor Filtration

Vapor filtration process aims to remove all solid particulates coming with the flow. Since all particle char are assumed to be completely separated in pyrolyzer, both cyclone and HGF only separate fine particulate matter of carbonaceous residues from pyrolysis. Cyclone removed 80% remaining solid while HGF eliminated the rest, as discussed in section 3.1.3. In addition to physical phase separation, coke is also assumed to form in HGF based on experiment results by Baldwin. Baldwin et al. observed additional thermal cracking and polymerization to form coke in HGF [53]. A further reaction occurred due to contact with hot surfaces in an extended period [35, 53]. Even though the rate of cracking is known to be substantially slower than cracking during pyrolysis reaction [53], the exact amount of coke formed is uncertain.

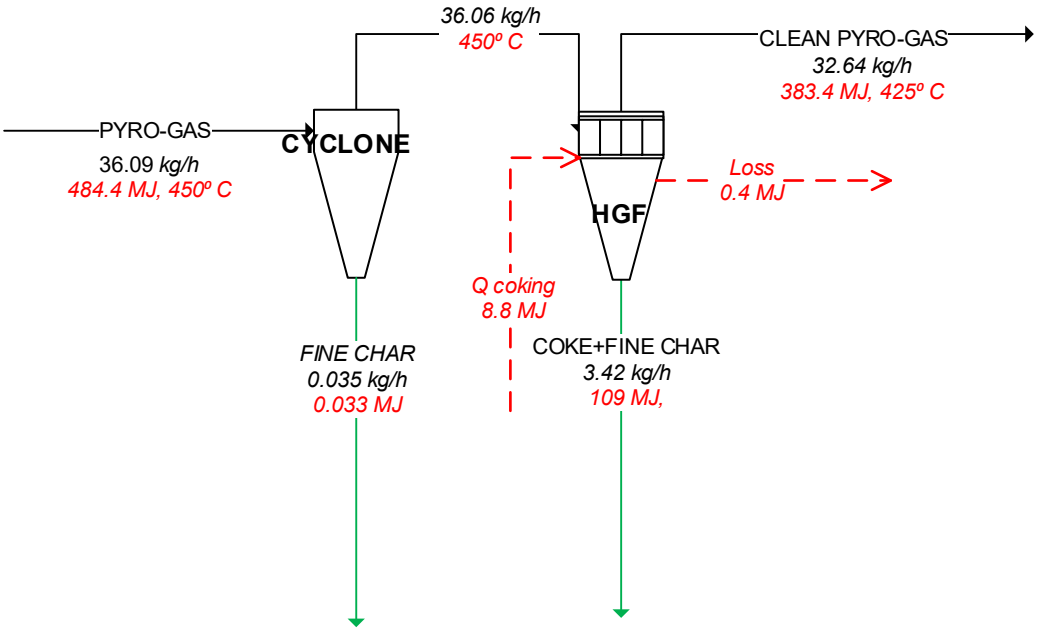

Figure 21 Mass and Energy (based on HHV) Balance in Cyclone and HGF

Due to this limitation, the mass of coke is roughly estimated. Mass of coke presented in Figure 21 follows the assumption taken by Dutta et al. [8]. The actual experiments revealed that coke formation required no extra energy from external sources. Thus, the heat consumption for coking is expected to be compensated by temperature decrease from pyrolysis outlet (450ºC) into upgrading temperature (425ºC). Nonetheless, Figure 21 captured the reaction still required extra heat to support the cracking reaction. Such result suggested the possibility of overestimation of the coke amount. Coke formation is inappropriately assumed since Dutta et al. performed simulation of vapor filtration in a different condition from this simulation.

4.1.4 Ex-situ Vapor Upgrading and Catalyst Regeneration

Figure 22 suggests that the upgrading process is slightly exothermic. The process reduced the weight of vapor phase product (Upgraded Gas) and generated 0.54 kg/h coke as the consequence of deoxygenation. The amount of coke formed, equal to 1.4% wt. of dry biomass, are more than five times lower than coke formed in in-situ upgrading [41]. In total, catalyst regeneration released 17.5 MJ heat or equal to 0.65 MJ/kg-dry vapor upgraded. However, this heat is unrecoverable in ex-situ practice.

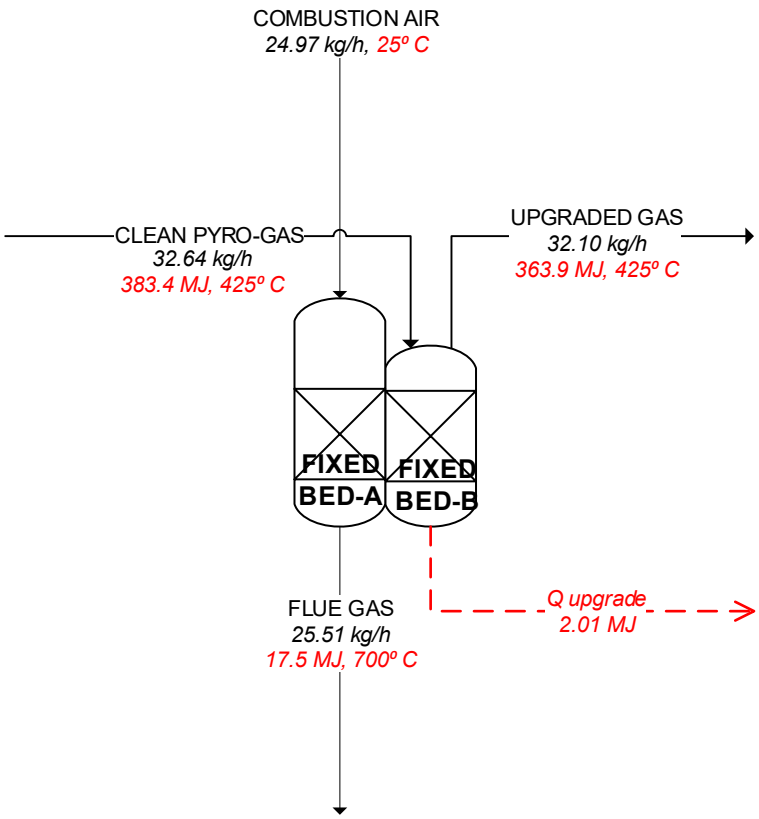

Figure 22 Mass and Energy (based on HHV) Balance in Fixed Bed Reactor

Several studies mentioned that deoxygenation reaction occurred in fixed bed reactor occurred via four distinct pathways: (1) decarbonylation removes oxygen as CO, (2) decarboxylation removes oxygen as CO_2, (3) hydrodeoxygenation and (4) a certain C-C reactions [8, 26]. Therefore, amounts of CO, CO_2, and H_2O are expected to increase. However, the simulation assumed the same composition of NCG before and after pyrolysis referring to experiment result by Bosong et al. [24] due to the limited data available. This assumption resulted in the energy release 50.26 kJ/kg-dry feed. Considering the possibility of inaccuracy assumption for NCG, the result is further compared to a study by Diebold et al.

Diebold et al. conducted ex-situ vapor upgrading of pinewood bio-oil in similar upgrading condition [26]. They observed vapor upgrading release 75 kJ/kg-dry oil, 50% higher than the simulation result. Besides different feedstock, such differences also possibly due to different NCG composition subsequent to upgrading process. NCG composition is then adjusted to investigate the significance of composition changes. Referring to upgrading mechanism, amount of CH_4, C_2+, and H_2 are modified to remain the same as NCG pyrolysis while amount of CO increase considering the elemental balance. As a result, the heat of reaction increase into 82 kJ heat released per kg-dry feed as summarized in Table 21. Due to such visible impact on heat of reaction, NCG composition ought to cautiously assume.

Table 21 Modification of NCG composition after vapor upgrading

Components	*NCG pyrolysis (kg/h)*	*NCG catalytic upgrade (kg/h)*	
		Initial data	*modified*
CH_4	0.421	0.543	0.421
C_2+alkane	0.239	0.308	0.239
CO	5.222	6.739	6.886
H_2	0.010	0.013	0.010
CO_2	8.767	11.313	11.313
Q upgrade from simulation [kJ/kg-feed]		-50	-82
Q upgrade reference (kJ/kg-feed)			-75 [26]

4.1.5 Vapor Quenching and Condensation

The vapor quenching and condensation process is aimed to separate the oil from permanent gas and prevent aging. In this process the bio-oil is also fractionized into HFO and LFO by implementing two scrubbers, i.e. HF and LF. The first scrubber HF aims to separate the heavy fraction from the light fraction oil. While the second scrubber LF aims to separate the light fraction oil from permanent gas (NCG). The optimum temperature of HF is 125°C while LF is 35°C. Two main criteria in determining optimum operating temperature of scrubbers are (1) to obtain highest oil yield possible with minimum moisture and (2) to minimize cooling oil requirement for the scrubber operation. Section 4.1.5.1 and 4.1.5.2 describe detail consideration for determining operating temperature of each scrubber.

The flow rate of each separated product summarized in Table 22. Flow rate differences between initial data, elaborated in section 3.2.2, and simulation result are less than 5% suggested that the quenching process is well performed. Such gaps occurred because organic contents of bio-oil partially escaped into NCG and water during separation.

Table 22 Product distribution from simulation vs. initial data

Products	*Flow rate (kg/h)*		*Difference*
	Original data	*Simulation result*	
Bio-oil	8.27	7.86	-4.96%wt.
Water	4.85	5.01	3.30%wt.
NCG	18.96	19.22	1.37%wt.

Figure 23 summarized all energy flows in the vapor quenching and condensation process. In total, this cooling process released 19.9 MJ and required 861.9 kg/h cooling oil. As described in section 3.1.5, upgraded gas is pre-cooled using the combustion air of NCG to minimize the amount of oil recirculation. This measure significantly lowered the recirculated HFO from more than 80 kg/h into 19.35 kg/h. Nevertheless, similar treatment is inapplicable to LFO since HF operated close to LFO dew point.

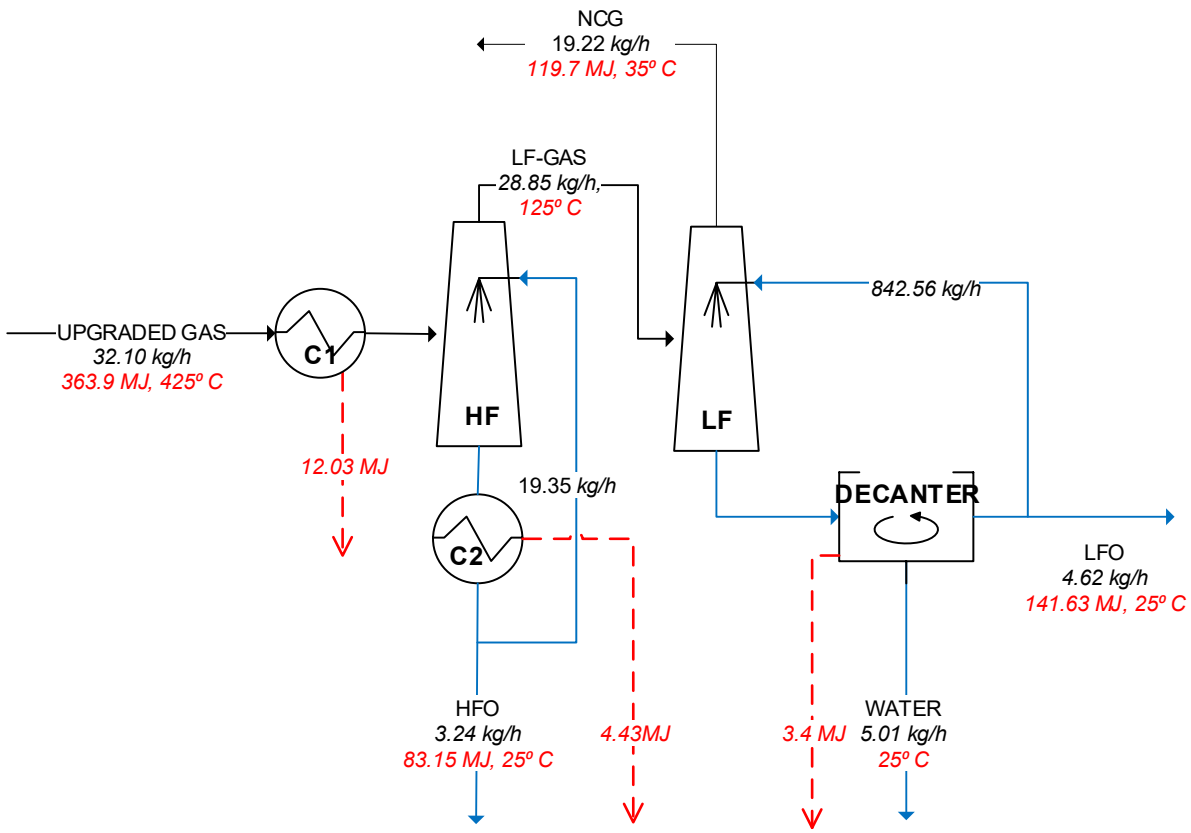

Figure 23Mass and Energy (based on HHV) Balance in Vapor Quenching Process

Numbers presented in Figure 23 are combination results of both simulation and manual calculation. The sum of heat flow (C1, C2, and DECANTER) is calculated by balancing the overall heat flow in manual calculation while heat for C1 and C2 specifically extracted from Aspen Plus simulation. Such measure is applied since those two methods derived different results. The total heat released from the manual calculation (19.9 MJ) is 20% lower from Aspen Plus (24.9 MJ) due to difference method applied during the simulation of bio-oil. As described in section 3.4 equation 19-21, empirical formulas are directly calculated enthalpy of bio-oil as vapor. In the other hand, Aspen Plus employs a model compound to represent bio-oil. However, such error is negligible since it is less than 1% of total heat involved in the whole system.

The HF scrubber recovered 41%wt. of bio-oil mass as HFO. This number is similar to practice by NREL which recover 40%wt. of its mass as HFO [6, 8]. Table 23 shows HFO comprised a higher oxygen content than LFO which led to a lower HHV. Most aromatics and water-soluble oxygenates in bio-oil are separated into LFO.

Table 23 HFO and LFO components

Parameters	*LFO*	*HFO*
Mass [kg/h]	4.62	3.24
Empirical formula	C_5H_5O	C_3H_3O
HHV dry (MJ/kg)	30.63	25.64
Components (%wt.)		
Acetol	7.2	0.6
Furfural	7.9	0.8
Dextrose	0	2.0
1,2-benzenediol	5.1	69.8
Guaiacol	51	22.4
o-xylene	7.6	0.2
1,2,3-trimethylbezene	6.8	0.2
2,6-dimethylnaphtalene	9.3	2.6
Indene	2.9	0.1
water	2.0	1.3

4.1.5.1 Determining the Operating Temperature of HF Scrubbers

Table 24 lists all organic components of the upgraded gas coming to the HF scrubbers. Simulation predicts the upgraded gas start to condense at 155ºC. Therefore, the HF scrubbers is simulated between range 100ºC-155ºC to investigate the effect of temperature on concentrations in HFO and the amount of condensed liquid. The temperature of 100ºC is selected as the bottom limit of the operating temperature to suppress moisture content of HFO. Even though the actual dew point of water is lower than 100ºC due to lower partial pressure, operating HF below 100ºC is avoided to completely eliminate the possibility of water presence. The water is expected to be condensed in LF then easily be separated from LFO in decanter.

Table 24 Organic components of inlet and outlet streams of HF and LF scrubbers

Composition	*Flow rate (kg/h)*			
	UPGRADED GAS (inlet HF)	*HFO*	*LF GAS (inlet LF)*	*LFO*
H_2O	4.864	0.042	4.822	0.092
Furfural	0.396	0.026	0.369	0.365
Acetol	0.354	0.019	0.335	0.333
Guaiacol	2.943	0.726	2.217	2.217
1,2-Benzenediol	2.951	2.262	0.686	0.236
Dextrose	0.066	0.065	< 0.001	< 0.001
o-xylene	0.616	0.006	0.611	0.351
1,2,3-Trimethylbenzene	0.329	0.006	0.324	0.314
2,6-dimethylnaphtalene	0.491	0.084	0.406	0.403
Indene	0.14	0.003	0.135	0.134

The first criteria of optimum temperature of scrubbers is to minimize the cooling oil demand for the overall quenching process. Operating HF at a lower temperature requires higher flow rate of cooling HFO due to the larger temperature difference between incoming Upgraded Gas and the HF operating temperature. Contrast to a higher demand for HFO cooling, a lower HF

temperature demands a lower LFO cooling. Assuming LF operates at constant temperature, a lower HF operating temperature decreases the temperature difference between HF outlet stream (LF gas) and LF operating temperature. The total demand of cooling oil for both HFO and LFO at varying HF temperature is depicted in Figure 24. Figure 24 indicates the demand for total cooling oil is linearly increase as HF temperature increase. Therefore, operating HF at a lower temperature is preferable from the demand of cooling oil perspective.

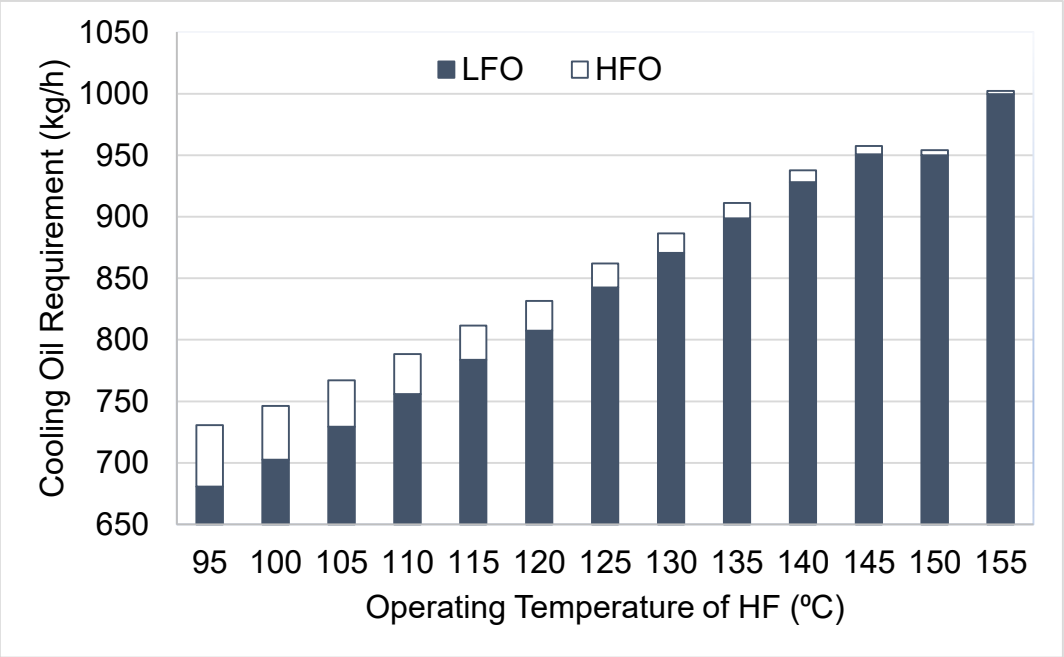

Figure 24 amount of cooling oil in various operating temperature of HF

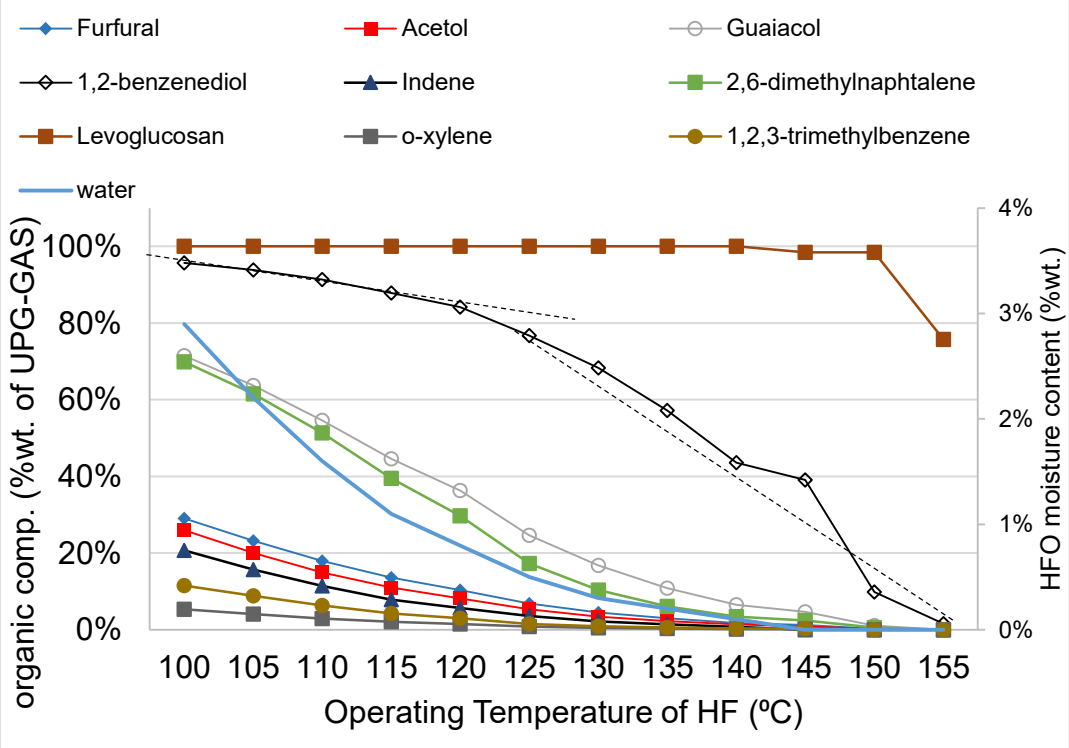

Figure 25 Separation quality of HFO component in various temperature of HF

The second criteria for the optimum temperature of HF scrubber is to obtain the highest yield of organic phase while minimize the moisture content of HFO. According to Figure 25, a lower operating temperature of HF also enhances the recovery of organic components of the oil. For example, operating HF at 120 °C recovers less than 40% wt. of 2,6-dimethylnaphtalene and guaiacol present in the Upgraded Gas. Whereas decreasing HF temperature into 100°C increases the recovery of those two component into more than 70% wt. However, the increasing rate of each component varies. For instances, 1,2-benzenediol increase at a relatively lower rate at temperature below 120°C compare to the yield increase between temperature range 125-155°C. In the other hand, lower temperature increase water content of the oil. The water content is remarkably increase at temperature below 125°C. As previously mentioned, the presence of water is avoided due to its detrimental effect. Since there is no decanter for HFO subsequent to HF scrubber, recirculating HFO as a cooling oil can potentially accumulate water. Considering the cooling oil demand, moisture content of HFO and the recovery of organic components, HF is decided to operate at 125°C. Such operating temperature condenses HFO with composition summarizes in Table 24.

4.1.5.2 Determining the Operating Temperature of LF Scrubbers

To investigate the optimum temperature, the LF is simulated at temperature range 30-50°C. This upper limit is selected based on other study conducted by Onarheim et al. [10]. As tabulated in Table 24, the light fraction gas reaching LF scrubber comprises seven organic compounds. The operation of LF aims to recover all of those organic components. Figure 26 reflects that operating LF at temperature higher than 40°C significantly decreases LFO recovery. Contrast to HF, water content is insignificant issue in determining operation temperature of LF since the LF is followed by decanter. In the other hand, the demand of LFO as cooling oil is remarkably increase at operating temperature below 35°C. Hence, LF operates at 35°C. At such temperature, the LF recovers 97% wt. of organic phase available from the gas reaching the LF scrubber.

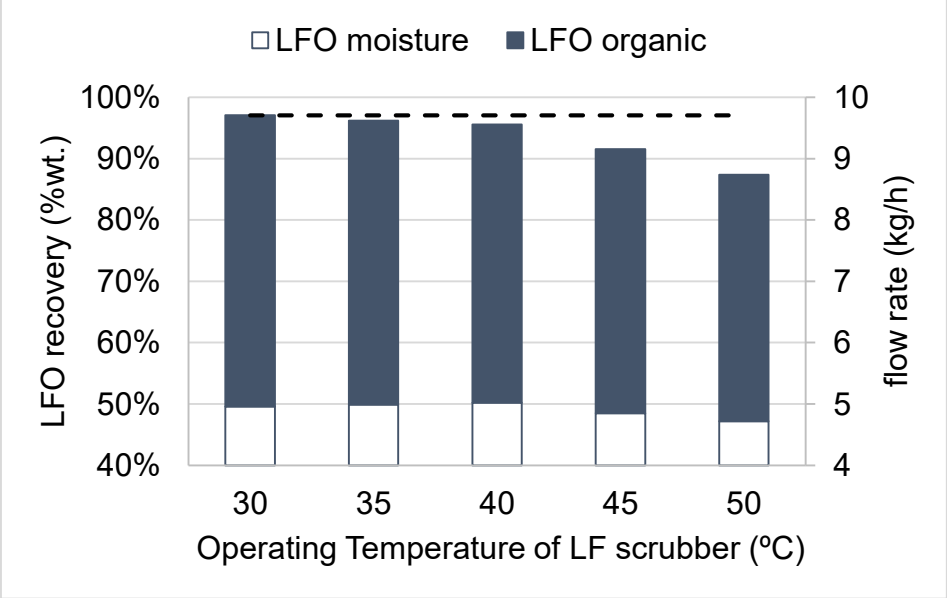

Figure 26 LFO recovery in various operating temperature of LF

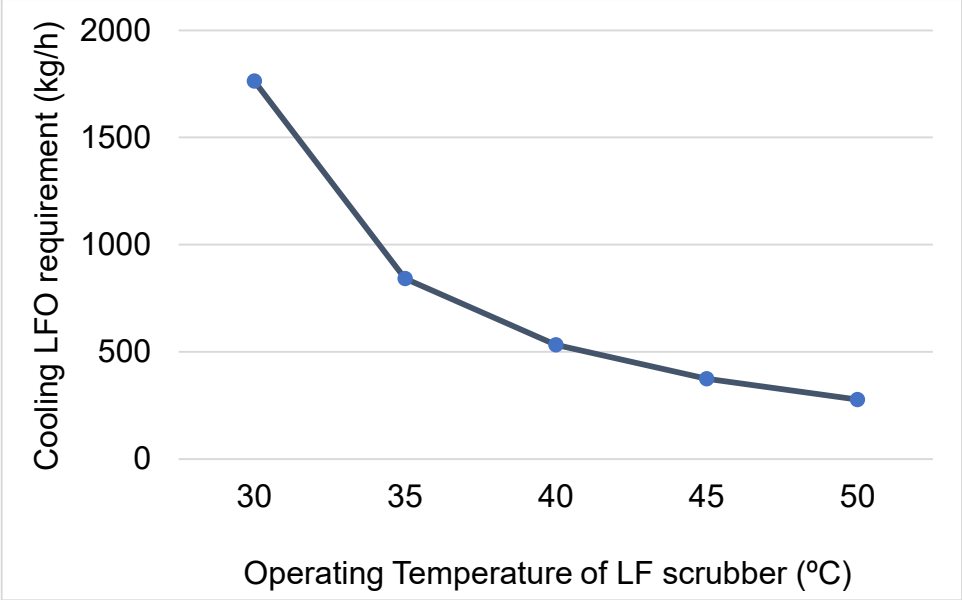

Figure 27 LFO cooling demand in various operating temperature of LF

4.1.6 Non-condensable Gas Combustion

Non-condensable gas produced during pyrolysis and upgrading processes is combusted to provide heat demand for drying. The combustion air is preheated using the heat recovered from HFO quenching. Note that energy provided for drying is almost three times higher than pyrolysis and NCG is unable to completely cover it. Extra 0.5 kg/h of methane is still required to maintain the flue gas temperature equal to 110ºC. Thus, biomass moisture is crucial properties and processing less moist biomass is obviously more preferable.

Interestingly, flue gas NCG for drying is exhausted at a relatively high oxygen content (19.6% vol.) and high temperature (60ºC). Hence re-combust exhaust gas in NCG combustor, instead of supplying fresh air for combustion, can be an improvement alternative. This scheme, depicted in Figure 29, suppressed heat consumption by 65.76 MJ or equal to cutting heat loss by 2.77%.

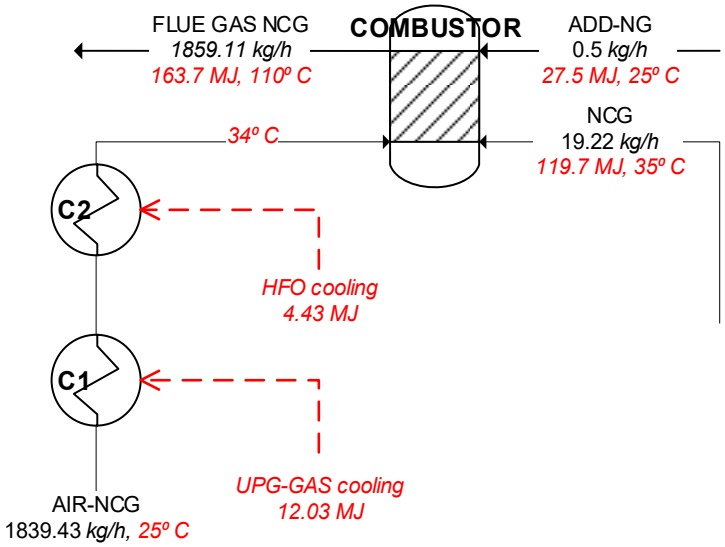

Figure 28 Mass and Energy (based on HHV) Balance in NCG Combustion

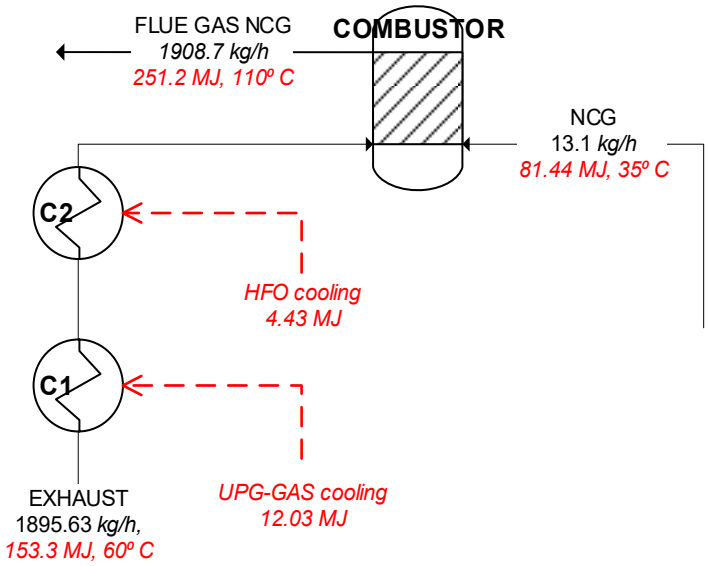

Figure 29 Suggested scheme for NCG combustion

4.1.7 Overall energy and Mass Balances

The summary of overall mass and energy balance of the overall process presented in this section as Sankey diagram in Figure 30 and Figure 31. In the mass balance, the amount of bio-oil is slightly decreased subsequent to vapor filtration due to the formation of coke. Further decrease of bio-oil is exposed after vapor upgrading due to oxygen removal [8]. Consequently, the amount of NCG and water increased. At the end of the process, biomass to bio-oil conversion is accounted for 19.65% wt. dry-biomass, NCG 48% wt., while char and coke 27.05% wt.

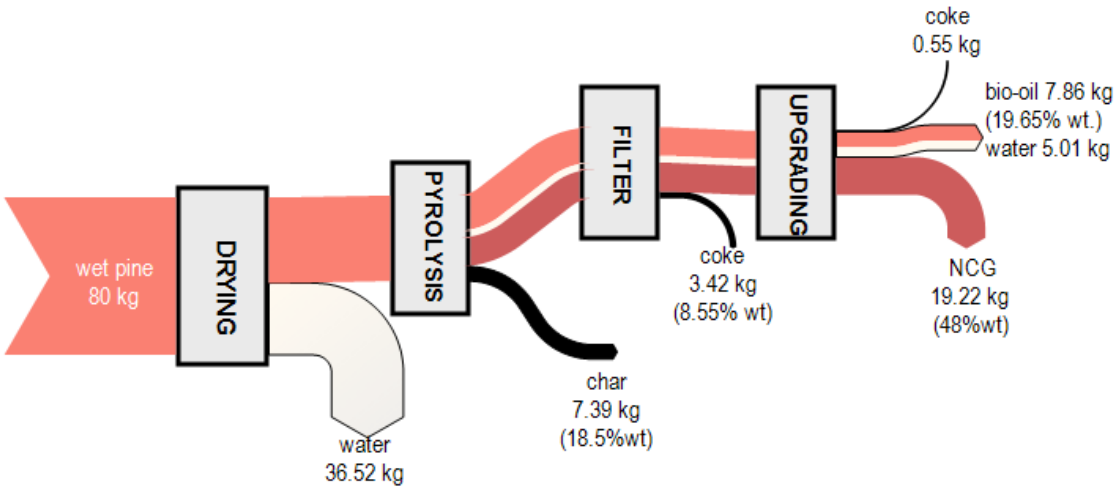

Figure 30 Sankey diagram of overall mass balance for 50%wt.MC feedstock

Energy balance depicted in Figure 31 illustrated the profile of input and output energy in whole system. Concerning energy output, solids dominated the energy content and accounted for more than 41% energy of all product. Bio-oil is 32.9% and NCG is the least, only 17.53%. Such numbers are attributed particularly to feedstock with moisture content 50%wt. The energy efficiency of bio-oil in varying moisture content is discussed further in section 4.2

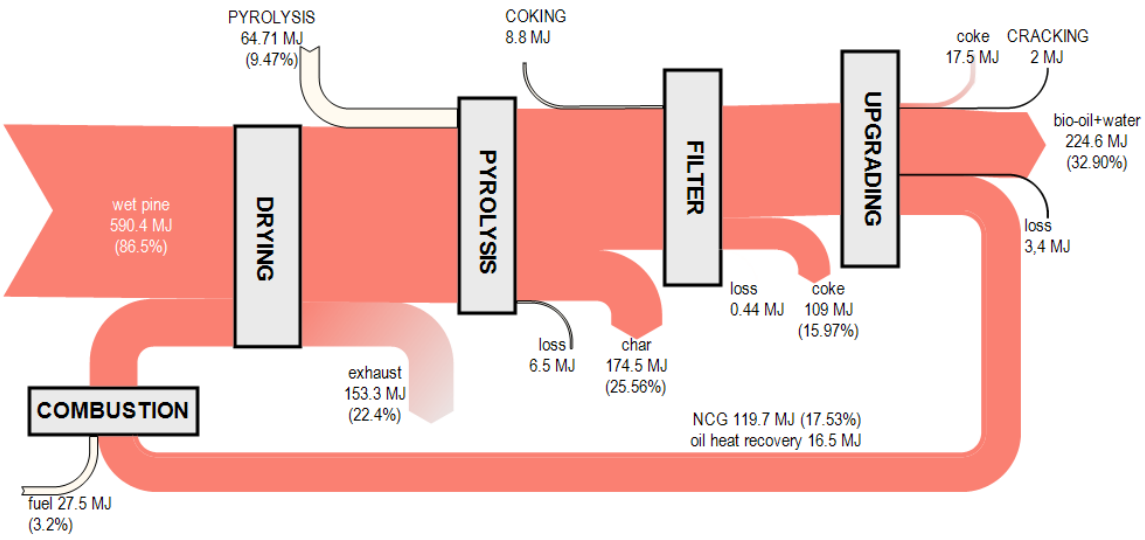

Figure 31 Sankey diagram of overall energy balance (based on HHV) for 50%wt.MC feedstock

In terms of energy input, pine is dominant supplier while heat for pyrolysis only contributed 9.47% of total energy.

4.2 Bio-oil Energy and Mass Efficiency

Mass and energy efficiency of bio-oil are two substantial parameters in a techno-economic analysis of bio-oil upgrading process as they reflected the amount of energy consumption and the amount of bio-oil production. Eventually, they economically affected the feasibility of the corresponding technology. Section 4.1.7 already mentioned that bio-oil mass and efficiency is 19.65%wt. and 32.90% respectively. However, those two parameters varied depending on several factors; this report investigated two of them: moisture content of feedstock and heat source for pyrolysis. The as-received moisture content of biomass is widely varied. In this report, moisture content is varied between range 10%-50%wt.

4.2.1 Effect of Moisture Content in Efficiency

Figure 32 showed that moisture content proportionally influenced the amount of bio-oil produced in an inverse-linear relationship. Total mass of bio-oil are linearly decreased by *ca.* 1.5 kg per 10%wt. moisture increase. It is evident that a higher moisture content of feedstock means a lower dry mass of feedstock. Dry mass of biomass linearly decrease 8 kg per 10%wt. moisture increase. Therefore, mass efficiency is constant at 19.6%wt. dry biomass regardless the moisture content. Amount of LFO is also always in constant proportion over HFO.

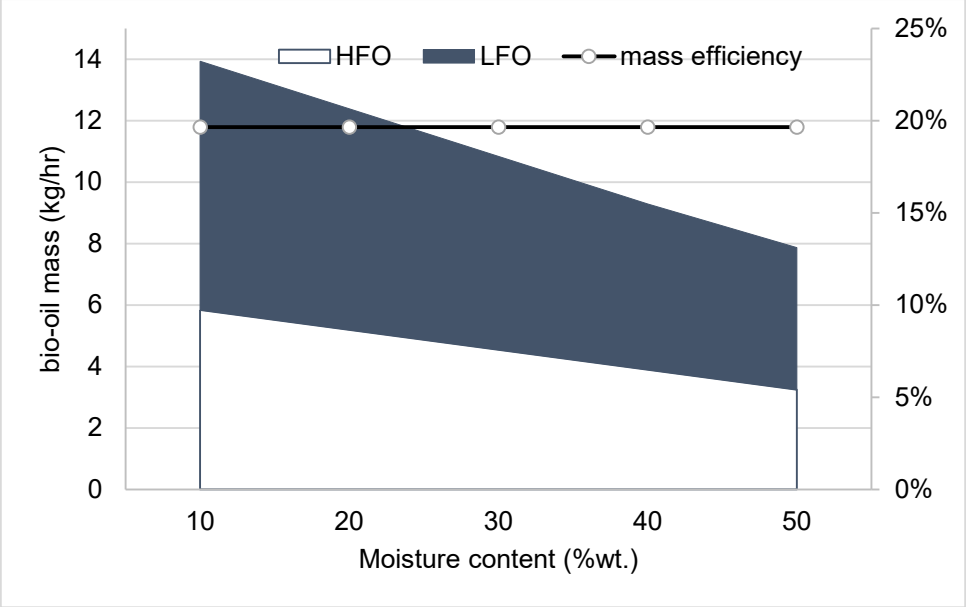

Figure 32 Effect of pinewood moisture content to the bio-oil mass flowrate

Unlike the constant mass efficiency, the energy efficiency of bio-oil increased as the moisture content decreased. Efficiency increased because the requirement of drying diminished with the decreasing moisture. Figure 33 captured the effect of moisture content to bio-oil energy efficiency. Two cases are investigated: (1) All NCG available, including the excess of the drying process, are utilized and (2) excess NCG is wasted. In general, utilizing all NCG excess increase efficiency approximately 1.38% increments per 10%wt. moisture content decrease. This excess calorie can be an alternative to partially substitute electricity consumption in pyrolyzer. Figure 34 exhibited that NCG excess even covered pyrolysis heat demand for feedstock with the moisture content lower than 30%wt., resulted in the possibility of a stand-alone process.

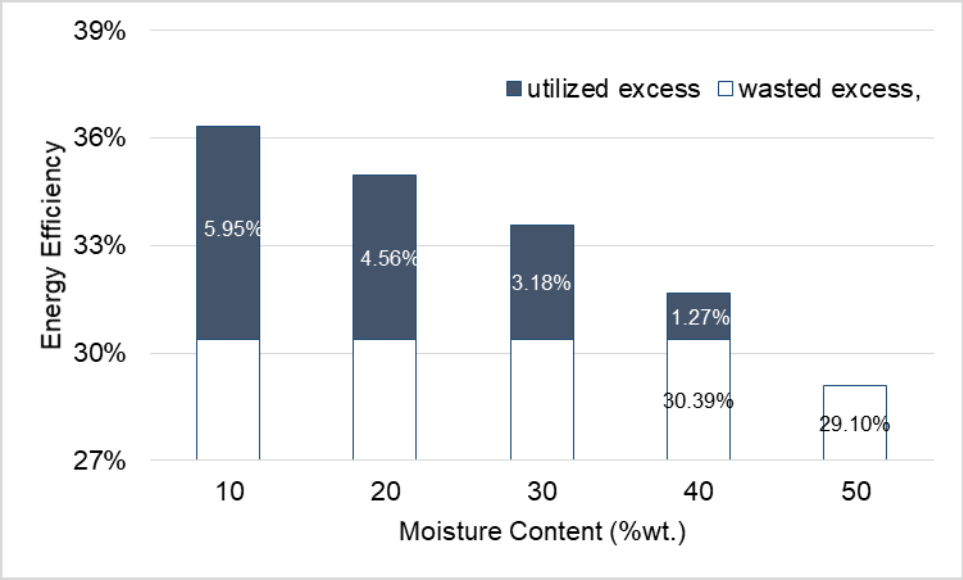

Figure 33 Effect of pinewood moisture content to bio-oil energy efficiency

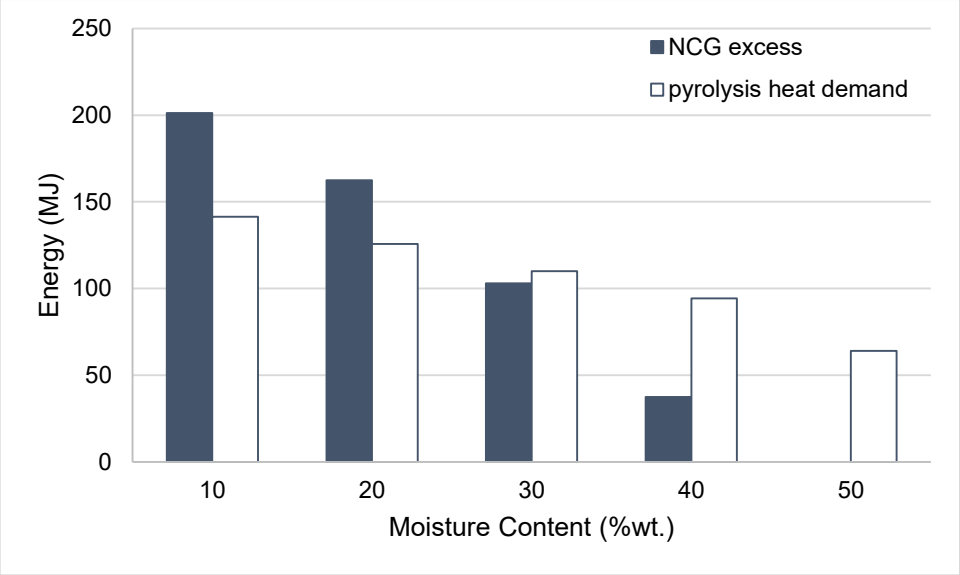

Figure 34 Amount of NCG excess vs. pyrolysis heat consumption in varying moisture content

4.2.2 Effect of Heat Source Type in Energy Efficiency of Bio-oil

As elaborated in section 2.4, most pyrolysis practices utilized thermal source for their pyrolysis process instead of electricity. This aspect is also the central character of in-situ pyrolysis: the pyrolysis heat is supplied by combusting coke and char. Interestingly, some char producers in Sweden preferred to use electric source because electricity is cheaper than char. This section aimed to investigate the effect of two type heat source to bio-oil energy efficiency in thermodynamic point of view.

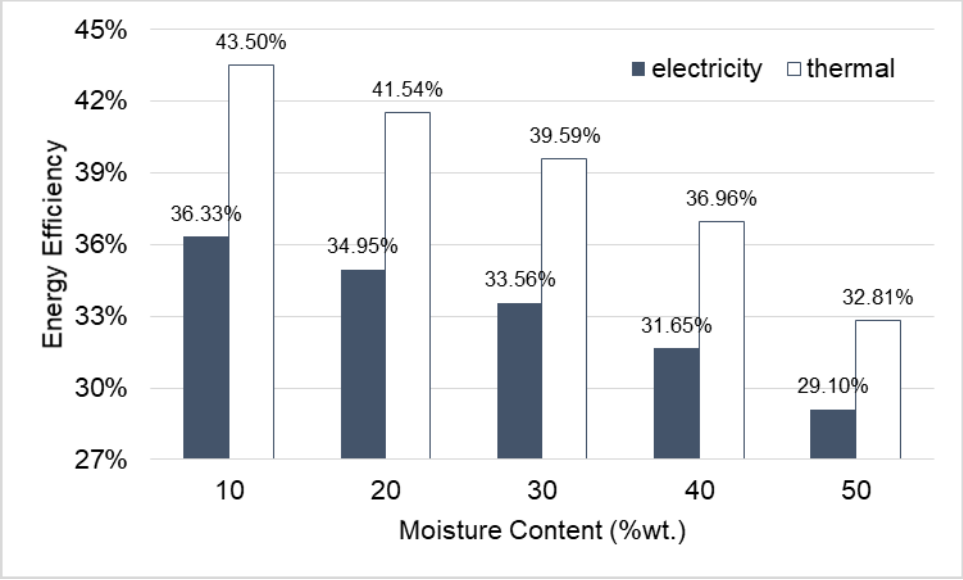

Figure 35 bio-oil energy efficiency in two different heating source of the pyrolyzer

As summarized in Figure 35, thermal heated pyrolysis process offered higher efficiency compared to electrical heated process due to energy conversion. The conversion decreased the efficiency proportionally to the heat of pyrolysis: a process which demanded the lowest pyrolysis heat yielded the least gap. Consequently, feedstock with 50%wt. moisture

demonstrated the lowest efficiency gap i.e. 32.81 vs. 29.10%. Hence, results suggested that electricity utilization in pyrolyzer is thermodynamically unpreferred.

Since NCG ranked as the lowest-value product, it is prioritized to be the thermal heat source. In case of NCG deficiency, the pyrolysis heat can be supplied by combusting the char. Moreover, char produced from this process is poor in quality, characterized by its low carbon content as tabulated in Table 25. However, further investigation on economic aspect is a necessity prior to confirming the utilization of char.

Table 25 Char elemental component of pinewood in various pyrolysis condition

Pyrolysis type	*Reactor*	*T (°C)*	*C*	*H*	*O*	*Ref*
Slow pyrolysis	Screw reactor	450	58.5	6.6	31.92	
	Fixed bed	300	54.1	5.9	40	[54]
		450	82.5	3.8	13.7	[54]
Fast pyrolysis	Fluidized bed	480	73.4	2.9	22.6	[10]

4.3 Economic Analysis

The profit of two scenarios, i.e. electricity-heating vs. char-heating pyrolysis unit are compared and results presented in Table 26 and Table 27 respectively. As tabulated in Table 26, income from bio-oil and char selling is almost evenly distributed. In term of expense, pine purchase dominated almost 75% of the total cost while electricity contributed the rest. In overall, the process yielded profit 1.47 SEK per kg dry feedstock. Interestingly, Table 27 captured that utilization of char as the heat source lowers the total profit since char is more expensive compared to electricity. Therefore, heating the pyrolysis by electricity is preferred despite its lower thermal efficiency.

Table 26 Profit of Ex-situ Catalytic Upgrading Process for electrical-heated Pyrolyzer

Variable	Quantity (per kg dry pine)		Unit Price		Cash Flow (SEK/kg dry pine)		
					Cost	Income	Profit
Pine	1	kg	0.787	SEK/kg	0.787		
Electricity	1.46	MJ	0.188	SEK/MJ	0.274		
Char	0.28	kg	4	SEK/kg		1.135	
Bio-oil	0.20	kg	7	SEK/kg		1.4	
Total					1.061	2.535	1.474

Table 27 Profit of Ex-situ Catalytic Upgrading Process for thermal- heated Pyrolyzer

Variable	Quantity (per kg dry pine)		Unit Price		Cash Flow (SEK/kg dry pine)		
					Cost	Income	Profit
Pine	1	kg	0.787	SEK/kg	0.787		
Char	0.20	kg	4	SEK/kg		0.8	
Bio-oil	0.20	kg	7	SEK/kg		1.4	
Total					0.787	1.2	1.41

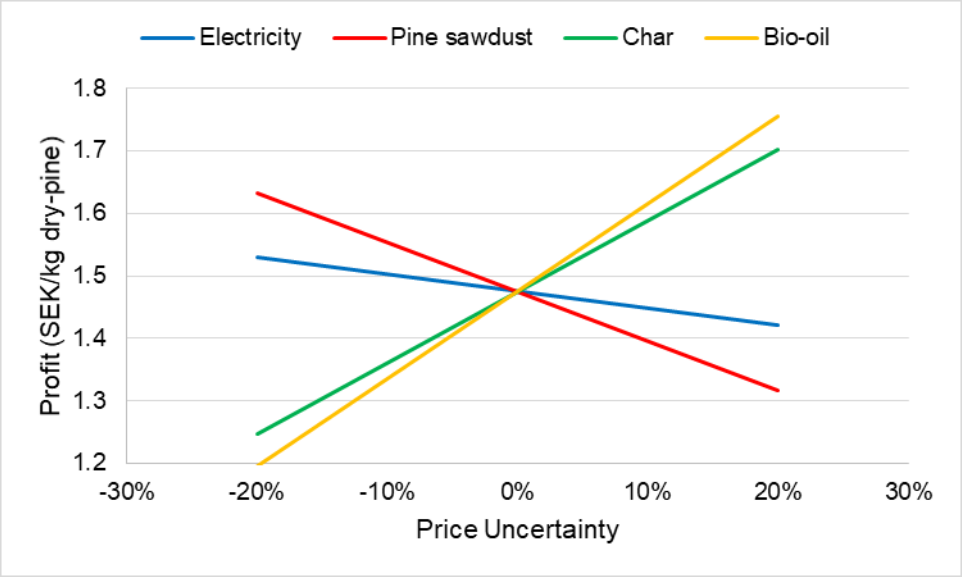

Figure 36 Effect of Price Uncertainty on Profit

Prices listed in Table 26 are the average value and actually varied over time. Figure 36 presents the sensitivity of profit with respect to price uncertainty. The sensitivity analysis is conducted in the range of -20% until 20% price variation to accommodate the real phenomenon. According to Swedish Energy Agency database, the industrial electricity price is maximum at 0.22 SEK/MJ and minimum 0.15 SEK/MJ during past 15 years [43]. As expected, least and highest variation caused by changes in electricity and bio-oil prices respectively. Such trends are proportional to the unit price of each material. Electricity possessed the cheapest unit price thus caused the lowest uncertainty, vice versa to bio-oil.

4.4 Comparison with Existing Upgrading Pathways

The performance comparison between ex-situ and in-situ catalytic upgrading is essential since ex-situ developed as an alternative solution of rapid catalyst deactivation of in-situ. As expected, the mass efficiency of bio-oil for in-situ is higher, almost 6%, than it is for simulation result of this work. It is reasonable since fast pyrolysis offered the highest yield of bio-oil among other types of pyrolysis. Both process produced a comparable amount of solids as shown in Table 28. Note char in catalytic fast pyrolysis is in contact with catalyst, thus risked to poison the catalyst.

Table 28 typical in-situ product yield distribution vs. simulation result

Products	*Yield Distribution (%wt. dry)*	
	In-situ [41]	*Ex-situ (this simulation)*
Bio-oil	24.3	19.65
NCG	21.3	48
Char-coke	25.3	28.42

Regarding energy, Figure 37 illustrated the heat balance of in-situ process with 80 kg/h feed at 50%wt. moisture content. Two most apparent differences between those two pathways are (1) in-situ consumed energy for pyrolysis 45% higher than result from this work and (2) in-situ is

a stand-alone process. The reason behind a higher pyrolysis energy consumption is similar to the discussion in section 4.1.2 about heat balance in pyrolyzer.

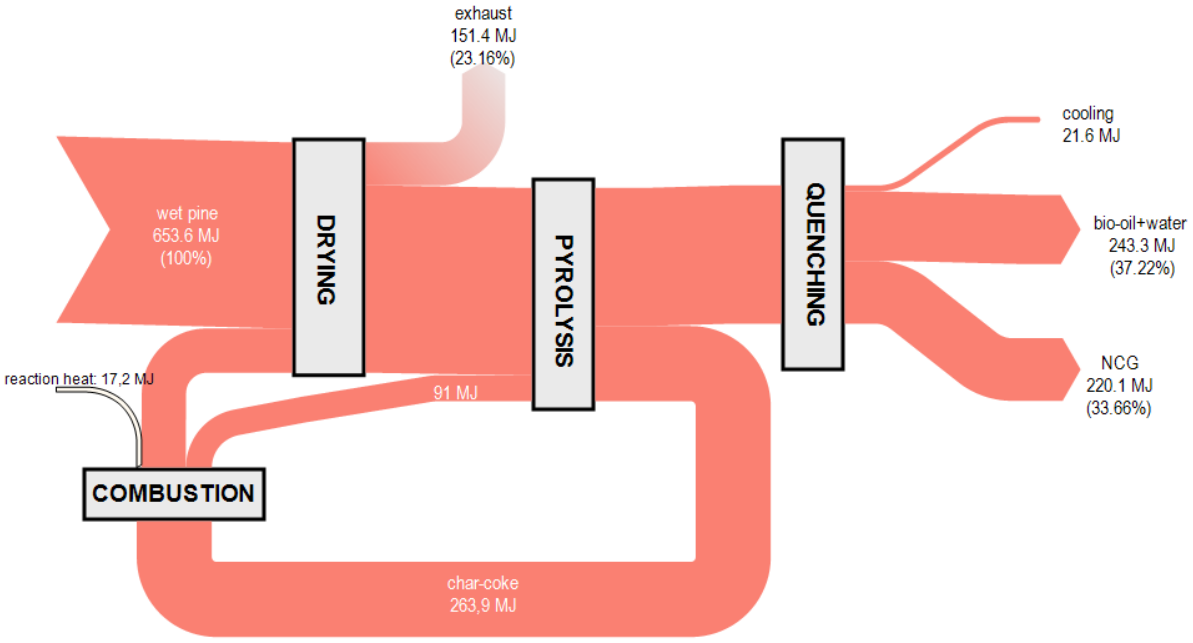

Figure 37 Overall energy balance of catalytic fast pyrolysis for 50%wt.MC feedstock [41, 55]

The second difference closely related to the particular characteristic of catalytic fast pyrolysis: coke and char in in-situ pathways are energy sources. Whereas coke covering catalyst is considered as heat loss in ex-situ, coke along with char covered the heat demand the in in-situ mechanism. Furthermore, char included as a commercial product in ex-situ. So, ex-situ relied solely on NCG as a heat source and on external energy source especially for feedstock with moisture higher than 30%wt.

Figure 37 also mentioned that energy efficiency of bio-oil in the in-situ scheme (37.22%) is higher than simulation result (32.81%). Note input energy for the in-situ scheme is only sourced from pine, energy efficiency of bio-oil supposed to be independent of moisture content. In the other hand, bio-oil energy efficiency varied according to the moisture content in ex-situ. Eventually, the energy efficiency of ex-situ is comparable to in-situ for moisture content 30%wt. or less, as mentioned in Table 29.

Table 29 Comparison of bio-oil mass and energy efficiency among upgrading technologies

Pyrolysis and Upgrading Type		T (ºC), P (bar)	η_{mass} (%wt.)	η_{en} (%)	Ref
Ex-situ	Slow pyrolysis- fixed bed catalytic	450, 1	19.6	39.6	
	Fast pyrolysis-fixed bed cat.-HP	500, 8.3	24	57	[8]
	Fast pyrolysis- HP	500, 1	36	50	[9]
	Mild catalytic pyro-HP	500, 1	17.7	39	[56]
In-situ	Fluidized bed	500, 1	25	39	[41]

Efficiency parameters of bio-oil owned by another ex-situ technologies combined with hydroprocessing (HP) listed in Table 29 demonstrated higher values in term of energy but comparable in term of mass. A slightly higher mass efficiency behavior potentially attributed to fast pyrolysis. Fast pyrolysis offered the highest liquid yield compared to other pyrolysis

pathways [12]. Whereas the higher energy efficiency possibly related to hydroprocessing characteristics. Hydroprocessing commonly generated process hydrogen from NCG [8, 9, 56], thus internally exploit the energy content of NCG instead of export it to neighboring process. Furthermore, hydroprocessing discharged oxygen as water [8, 9, 56]. This mechanism prevented the loss of carbon content, which also represented energy content, of bio-oil.

5 CONCLUSION

5.1 Conclusion

Analysis of simulation result presented in previous chapters can be concluded as follow:

1. The energy content of NCG available from the process is lower than the demand for drying feedstock from 50%wt. into 8%wt. moisture content, so the process required additional 0.5 kg/h methane. Reducing the biomass moisture content into 40% eliminate the requirement of additional fuel.
2. Slow pyrolysis of pinewood sawdust in screw reactor at 450ºC consumed 1.46 MJ/kg dry-feed (excluding the energy loss).
3. The deoxygenation process of pyrolysis vapor in fixed-bed reactor releases 50kJ/kg dry-feed
4. The conversion of biomass into bio-oil in dry basis possesses mass efficiency of 19.65%wt. while energy efficiency of oil 29.10% (based on HHV). The energy efficiency raised to 32.81% if direct thermal source applied instead of an electric heater. However, electrically-heated pyrolysis unit offers a better profit.
5. Decreasing moisture content by 10% increased bio-oil energy efficiency by 1.38%, the energy content of NCG covered energy demand of both pyrolysis and drying at moisture content less than 30%wt.
6. In average, bio-oil and char production in ex-situ catalytic upgrading generated profit 1.47 SEK/kg dry-feed. The uncertainty of bio-oil price caused the highest profit variation.
7. Ex-situ catalytic upgrading provides a comparable bio-oil energy and mass efficiency to existing in-situ catalytic upgrading technology.

5.2 Recommendation for future study

Due to the lack of data available, data inputted to simulation are sourced from several separated studies. Thus, this simulation is subjected to inaccuracy. It is recommended to validate results with experiments.

6 REFERENCES

[1] E. Kantarelis, "Catalytic Steam Pyrolysis of Biomass for Production of Liquid Feedstock: Doctoral Dissertation," Royal Institute of Technology, Stockholm, 2014.

[2] D. Elliott, T. Hart, G. Neuenschwander, L. Rotness, M. Olarte, A. Zacher and Y. Solantausta, "Catalytic hydroprocessing of fast pyrolysis bio-oil from pine sawdust.," *Energy Fuels,* vol. 26, no. 6, pp. 3891-3896., 2012.

[3] H. Wang, J. Male and Y. Wang, "Recent advances in hydrotreating of pyrolysis bio-oil and its oxygen-containing model compounds," *ACS Catalysis,* vol. 3, no. 5, pp. 1047-1070., 2013.

[4] A. Zacher, M. Olarte, D. Santosa, D. Elliott and S. Jones, "A review and perspective of recent bio-oil hydrotreating research," *Green chemistry,* vol. 16, no. 2, pp. 491-515, 2014.

[5] A. Gayubo, A. Aguayo, A. Atutxa, B. Valle and J. Bilbao, "Undesired components in the transformation of biomass pyrolysis oil into hydrocarbons on an HZSM-5 zeolite catalyst," *J. Chem. Technol. Biotechnol,* vol. 80, no. 11, pp. 1244-1251, 2005.

[6] A. Dutta, A. Sahir, E. Tan, D. Humbird, L. J. Snowden-Swan, P. Meyer, J. Ross, D. Sexton, R. Yap and J. Lukas, "rocess Design and Economics for the Conversion of Lignocellulosic Biomass to Hydrocarbon Fuels," National Renewable Energy Laboratory, Colorado, March 2015.

[7] J. Brown and R. Brown, "Process optimization of an auger pyrolyzer with heat carrier using response surface methodology," *Bioresource Technology,* vol. 103, no. 1, p. 405–414., 2012.

[8] A. Dutta, J. A. Schaidle, D. Humbird and F. G. Baddour, "Conceptual Process Design and Techno-Economic Assessment of Ex Situ Catalytic Fast Pyrolysis of Biomass: A Fixed Bed Reactor Implementation Scenario for Future Feasibility," *Topics in Catalysis,* vol. 59, no. 1, p. 2–18, January 2016.

[9] M. Wright, D. Daugaard, J. Satrio and R. Brown, "Techno-economic analysis of biomass fast pyrolysis to transportation fuels," *Fuel,* vol. 89, pp. S2-S10, 2010.

[10] K. Onarheim, Y. Solantausta and J. Lehto, "Process Simulation Development of Fast Pyrolysis of Wood Using Aspen Plus," *Energy & Fuels,* vol. 29, no. 1, pp. 205-217, Jan 15, 2015.

[11] H. Yang, S. Kudo, H.-P. Kuo, K. Norinaga, A. Mori, O. Masek and J.-i. Hayashi, "Estimation of Enthalpy of Bio-Oil Vapor and Heat Required for Pyrolysis of Biomass," *Energy Fuels,* vol. 27, p. 2675−2686, 2013.

[12] M. I. Jahirul, M. G. Rasul, A. A. Chowdhury and N. Ashwath, "Biofuels Production through Biomass Pyrolysis—A Technological Review," *Energies ,* vol. 5, no. 12, pp. 4952-5001, 2012, .

[13] C. Hu, R. Xiao and H. Zhang, "Ex-situ catalytic fast pyrolysis of biomass over HZSM-5 in a two-stage fluidized-bed/fixed-bed combination reactor," *Bioresource Technology,* vol. 243, p. 1133–1140, 2017.

[14] M. Balat, M. Balat, E. Kirtay and H. Balat, "Main routes for the thermo-conversion of biomass into fuels and chemicals. Part 1: Pyrolysis systems," *Energy Conv. Manag,* vol. 50, p. 3147–3157, 2009.

[15] T. Bridgwater, "Pyrolysis of Biomass. IEA Bioenergy: Task 34," Bioenergy Research Group, Aston University, Birmingham, UK, 2007.

[16] Y. Li, B. Li, X. Zhang, L. Chen, Q. Zhang, T. Wang and L. Ma, "Continuous pyrolysis and catalytic upgrading of corncob hydrolysis residue in the combined system of auger reactor and downstream fixed-bed reactor," *Energy Conversion and Management,* vol. 122, pp. 1-9, 15 August 2016.

[17] V. Guda and H. Toghiani, "Altering bio-oil composition by catalytic treatment of pine wood pyrolysis vapors over zeolites using an auger - packed bed integrated reactor system," *Biofuel Research Journal,* vol. 11, pp. 448-457, 2016.

[18] G. Zhou, P. A. Jensen, D. M. Le, N. O. Knudsen and A. D. Jensen, "Direct upgrading of fast pyrolysis lignin vapor over the HZSM-5 catalyst," *Green Chem,* vol. 18, p. 1965–1975 , 2016.

[19] S. Stefanidis, K. Kalogiannis, E. Iliopoulou, A. Lappas and P. Pilavachi, "In situ upgrading of biomass pyrolysis vapors: catalyst screening on a fixed bed reactor," *Bioresource Technology,* vol. 102, p. 8261–8267., 2011.

[20] Q. Lu, Y. Zhang, Z. Tang, W. Li and X. Zhu, "Catalytic upgrading of biomass fast pyrolysis vapors with titania and zirconia/titania based catalysts," *Fuel,* vol. 89, p. 2096–2103, 2010.

[21] Y. Zhao, L. Deng, B. Liao, Y. Fu and Q. Guo, "Aromatics production via catalytic pyrolysis of pyrolytic lignins from bio-oil," *Energy Fuel,* vol. 24, p. 5735–5740, 2010.

[22] S. Kersten, W. V. Swaaij, L. Lefferts and K. Seshan, "Options for catalysis in the thermochemical conversion of biomass into fuels," in *Catalysis for Renewables: From Feedstock to Energy Production*, Weinheim, WileyVCH Verlag GmbH & Co. KGaA, 2007, p. 119–147.

[23] G. Yildiz, M. Pronk, M. Djokic, K. van Geem, F. Ronsse, R. van Duren and W. Prins, "Validation of a new set-up for continuous catalytic fast pyrolysis of biomass Validation of a new set-up for continuous catalytic fast pyrolysis of biomass," *Journal of Analytical and Applied Pyrolysis,* vol. 103, p. 343–351, 2013.

[24] B. Li, W. Lu, Q. Zhang, T. Wang and L. Ma, "Pyrolysis and catalytic upgrading of pine wood in a combination of auger reactor and fixed bed," *Fuel,* vol. 129, pp. 61-67, 1 August 2014.

[25] J. N. Brown, "Development of a lab-scale auger reactor for biomass fast pyrolysis and process optimization using response surface methodology: Graduate Theses and Dissertation," Iowa State University, 2009.

[26] J. P. Diebold, "Catalytic upgrading of biocrude oil vapors to produce hydrocarbons for oil refining applications," National Renewable Energy Laboratory, Golden, Colorado, 1994.

[27] L. Jeczmionek and K. Porzycka-Semczuk, "Hydrodeoxygenation, decarboxylation and decarbonylation reactions while co-processing vegetable oils over a NiMo hydrotreatment catalyst.Part I: Thermal effects – Theoretical considerations," *Fuel,* vol. 131, pp. 1-5, 2014.

[28] L. Xu, Y. Zhang and Y. Fu, "Advances in Upgrading Lignin Pyrolysis Vapors by Ex Situ Catalytic Fast Pyrolysis," *Energy Technology,* vol. 5, pp. 30-51, 2017.

[29] K. Iisa, R. J. French, K. A. Orton, M. M. Yung, D. K. Johnson, J. ten Dam, M. J. Watson and M. R. Nimlos, "In Situ and ex Situ Catalytic Pyrolysis of Pine in a Bench-Scale Fluidized Bed Reactor System," *Energy and Fuels,* vol. 30, no. 3, p. 2144–2157, 2016.

[30] M. Asadieraghi and W. Daud, "In-situ catalytic upgrading of biomass pyrolysis vapor: Using a cascade system of various catalysts in a multi-zone fixed bed reactor," *Energy Conversion and Management,* vol. 101, pp. 151-163, 2015.

[31] F. Scala, Fluidized Bed Technologies for Near-Zero Emission Combustion and Gasification, Woodhead, 2013.

[32] A. Bridgwater and G.V.CPeacocke, "Fast pyrolysis processes for biomass," *Renewable and Sustainable Energy Reviews,* vol. 4, no. 1, pp. 1-73, March 2000.

[33] S. M. Walas, "Chapter 9: Dryer and Cooling Tower," in *Chemical Process Equipment: Selection and Design*, Newton, MA, Butterworth-Heninemann Series in Chemical Engineering, 1990, p. 243.

[34] J. Koppejan, S. v. Loo, Taylor and Francis, "Biomass Fuel Supply and Pretreatment," in *The Handbook of Biomass Combustion and Co-firing*, 2007, pp. 54-107.

[35] M. Ringer, V. Putsche and J. Scahill, "Large-Scale Pyrolysis Oil Production: A TechnologyAssessment and Economic Analysis," National Renewable Energy Laboratory, Golden, Colorado, 2006.

[36] X. Wang, "Biomass Fast Pyrolysis in a Fluidized Bed. Ph.D. Thesis," University of Twente, Enscheda, The Netherlands, 2006.

[37] X. Wang, S. Kersten, W. Prins and W. Van Swaaij, "Biomass pyrolysis in a fluidized bed reactor. Part 2: Experimental Validation of Model Results," *Ind. Eng. Chem. Res. ,* vol. 44, p. 8786–8795, 2005.

[38] Kilpinen and Zevenhoven, "Chapter 5 Particulate," in *Control of pollutants in flue gases and fuel gases*, 2004, pp. 1-32.

[39] J. V. J. Klingspor, "Particulate control for coal combustion," IEA Coal Research, London, 1988.

[40] S. Mitchell, "Hot gas particulate filtration," IEA Coal Research, London, 1997.

[41] E. Birru, A. Martin, C. Erlich, W. Yang, R. Pellny, T. Ekbom, N. Padban and C. Gustavsson, "Technical and Economical Potential for Combined Heat, Power and Bio-Oil Production In Power Plants-CHPO," Stockholm, 2015.

[42] L. Ingram, D. Mohan, M. Bricka, P. Steele, D. Strobel, D. Crocker, B. Mitchell, J. Mohammed, K. Cantrell and C. U. J. Pittman, "Pyrolysis of Wood and Bark in an Auger Reactor: Physical Properties and Chemical Analysis of the Produced Bio-oils," *Energy and Fuels,* vol. 62, no. 1, pp. 614-625, 2008.

[43] S. E. Agency, "Statistic Sweden," Statistics Sweden's Switchboard, 13 February 2018. [Online]. Available: http://www.scb.se/en/finding-statistics/statistics-by-subject-area/energy/price-trends-in-the-energy-sector/energy-prices-on-natural-gas-and-electricity/pong/tables-and-graphs/average-prices-by-half-year-2007/prices-on-electricity-for-industrial-consumers. [Accessed 25 May 2018].

[44] R. Sharma, J. Wooten, V. Baliga, X. Lin, W. Chan and M. Hajaligol, "Characterization of chars from pyrolysis of lignin," *Fuel,* vol. 83, p. 1469–1482., 2004.

[45] J. R. Couper, W. Penney, J. R. Fair and S. M. Walas, "Gas-Solid Separation," in *Chemical Process Equipment Selection and Design, 2nd edition*, Burlington, MA, Elsevier, 2005, pp. 693-718.

[46] X. Ren, J. Meng, J. Chang, S. S. Kelley, H. Jameel and S. Park, "Effect of blending ratio of loblolly pine wood and bark on the properties of pyrolysis bio-oils," *Fuel Processing Technology,* vol. 167, p. 43–49, 2017.

[47] S. Thangalazhy-Gopakumar, S. Adhikari, H. Ravindran, R. B. Gupta, O. Fasina, M. Tu and S. D. Fernando, "Physiochemical properties of bio-oil produced at various temperatures from pine wood using an auger reactor," *Bioresource Technology,* vol. 101, no. 21, pp. 8389-8395, 2010.

[48] I. Aspen Technology, "Getting Started Modeling Processes with Solids," Aspen Technology, Inc, Burlington, MA, 2013.

[49] A. Gooty, D. Li, C. Briens and F. Berruti, "Fractional condensation of bio-oil vapors produced from birch bark pyrolysis," *Separation and Purification Technology,* vol. 124, pp. 81-88, 2014.

[50] R. Perry and D. Green, "Physical and Chemical Data," in *Perry's Chemical Engineers' Handbook, 7th edition*, McGraw-Hill, 1999.

[51] I. Aspen Technology, "Aspen Physical Property System: Physical Property Methods," Aspen Technology, Inc., Burlington, MA, 2013.

[52] F. Trippe, M. Fröhling, F. Schultmann, R. Stahl and E. Henrich, "Techno-Economic Analysis of Fast Pyrolysis as a Process Step Within Biomass-to-Liquid Fuel Production," *Waste and Biomass Valorization,* vol. 1, no. 4, pp. 415-430, 2010.

[53] R. Baldwin and C. Feik, "Bio-oil Stabilization and Upgrading by Hot Gas Filtration," *Energy Fuels,* vol. 27, no. 6, pp. 3224-3238, 2013.

[54] F. Ronsse, S. van Hecke, D. Dickinson and W. Prins, "Production and characterization of slow pyrolysis biochar: influence of feedstock type and pyrolysis conditions," *GCB Bioenergy,* vol. 5, no. 2, 2012.

[55] J. Guzman, "Process Design and Technical Feasibility Analysis of Catalytic Fast Pyrolysis for Biocrude Production, Master Thesis," Royal Institute of Technology, Stockhol, 2017.

[56] R. Thilakaratne, T. Brown, Y. Li, G. Hu and R. Brown, "Mild catalytic pyrolysis of biomass for production of transportation fuels: a techno-economic analysis," *Green Chemistry,* vol. 16, no. 2, pp. 627-636, 2014.

[57] A. Bridgwater, "Fast pyrolysis of biomass for the production of liquids," in *Biomass combustion science, technology and engineering, Chapter 7*, Woodhead Publishing Limited, 2013, pp. 130-171.

[58] Y. Wang and J. Wang, "Multifaceted effects of HZSM-5 (Proton-exchanged Zeolite Socony Mobil-5) on catalytic cracking of pinewood pyrolysis vapor in a two-stage fixed bed reactor," *Bioresource Technology ,* vol. 214, p. 700–710, 2016.

APPENDIX 1

The overall Aspen Plus Model

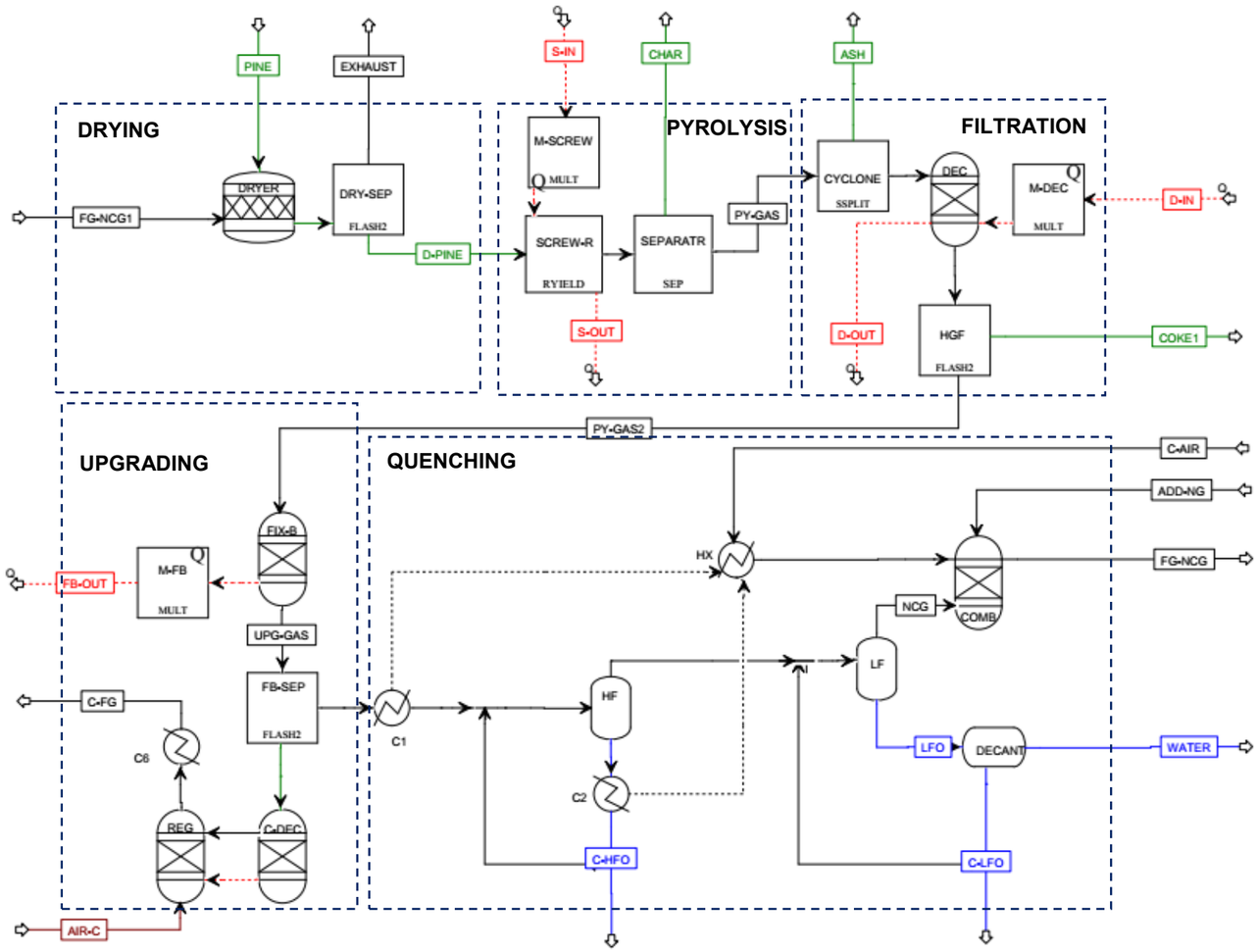

APPENDIX 2

Mass flow rate of streams

Mass Flow (kg/h)	EXHAUST	PY-GAS	PY-GAS2	UPG-GAS	C-FG	UPG-G1	REC-HFO	LF-GAS	REC-LFO	NCG	FG-NCG	WATER
Total	1895.633	36.058	32.639	32.097	4.982	32.097	19.354	28.852	842.407	19.234	1859.112	5.059
H_2O	40.24	3.419	3.419	4.864	0.673	4.864	0.248	4.822	13.807	0.066	3.067	4.682
Furfural		0.267	0.216	0.396		0.396	0.159	0.369	65.617	0.028		< 0.001
Acetol		0.74	0.599	0.354		0.354	0.11	0.335	59.715	0.022		0.004
Guaiacol			2.402	2.943		2.943	4.328	2.217	422.708	0.012		< 0.001
1,2-Benzenediol		2.107	1.706	2.951		2.951	13.507	0.686	48.018	< 0.001		0.373
Vanila		2.22	1.797									
Benzoic acid		0.06	0.049									
Dextrose		9.334	7.557	0.066		0.066	0.395	< 0.001	0.001	trace		< 0.001
Oleic acid		0.26	0.211									
CH_4		0.421	0.42	0.543		0.543	< 0.001	0.543	0.012	0.542		trace
C_2H_6		0.099	0.099	0.128		0.128	< 0.001	0.128	0.02	0.128		trace
C_2H_4		0.139	0.14	0.18		0.18	< 0.001	0.18	0.019	0.18		trace
C_6H_6		0.036	0.036	0.047		0.047	0.001	0.047	1.847	0.036		trace
CO_2	27.887	8.761	8.761	11.305	0.514	11.305	0.005	11.304	2.018	11.293	26.374	< 0.001
CO		5.218	5.219	6.734	0.378	6.734	< 0.001	6.734	0.034	6.734		trace
H_2		0.01	0.01	0.012		0.012	trace	0.012	< 0.001	0.012	trace	trace
O_2	416.441				0.005						418.673	
N_2	1411.066				3.405						1410.997	
C												

Mass Flow (kg/h)	EXHAUST	PY-GAS	PY-GAS2	UPG-GAS	C-FG	UPG-G1	REC-HFO	LF-GAS	REC-LFO	NCG	FG-NCG	WATER
Phenol		2.968										
o-xylene				0.616		0.616	0.031	0.611	70.281	0.143		trace
Trimethylbenz.				0.329		0.329	0.033	0.324	56.323	0.029		trace
2,6-dimethylnaph				0.491		0.491	0.508	0.406	77.612	0.001		trace
Indene				0.140		0.14	0.028	0.135	24.376	0.008		trace
NO					0.008							
NO_2					trace							

APPENDIX 3

1. Manual Calculation for Heat of Pyrolysis

Bio oil	*MW*	*mass flow rate (kg/h)*	*Moles flow rate (kmol/h)*	*ratio (/C)*
C	12	9.462	0.79	1.00
H	1	1.353	1.35	1.72
O	16	7.101	0.44	0.56
Bio oil enthalpy of formation [kJ/kmol-C]				-105,354
Bio oil sensible heat at 450°C [kJ/kmol]				26,369

Flue gas product				*H°f flue gas[kJ/h]*	
Composition	*H°f [kJ/kmol]*	*Pine*	*Char*	*Pine*	*Char*
CO_2	-393,510	1.6	0.36	-625,681	-141,804
H_2O	-241,814	1.0	0.25	-241,814	-59,215
$H°_f$ combustion product				-867,495	-201,019

Parameter	*Unit*	*Pine*	*Char*
Mass flow rate (dry-mass)	[kg/h]	40	7.39
HHV dry-mass	[kJ/kg]	14,761	23,533
	[kJ/h]	589,830	173,942
$H°_f$	[kJ/h]	-277,665	-27,077
ΔH (T)	[kJ/h]	1,755	7,022

Element	*MW*	*Flow rate*		*Pyrolysis Output*		*Pyrolysis Input*
		[kg/h]	*kmol/h*	*H (450°C) [kJ/kmol]*	*H(450°C) [kJ/h]*	*H (60°C) [kJ/h]*
CO	28	5.22	0.187	-97,723	-18,226	
CO_2	44	8.77	0.199	-374,503	-74,623	
CH_4	16	0.42	0.026	-40,569	-1,067	
C_2H_4	27	0.24	0.009	181,894	1,626	
H_2	2	0.01	0.005	12,486	61	
H_2O (vapor)	18	3.42	0.190	-226,677	-43,101	
Bio oil		17.92	0.789	-78,985	-62,281	
Char		7.39			-20,055	
Biomass		40				-275,909
Total enthalpy					-217,667	-275,909

Ideal energy requirement for pyrolysis 58,243 [kJ/h]

2. Manual Calculation for Heat of Coke Formation in HGF

Bio oil	*inlet 450°C*	*Outlet 425°C*
C ratio respect to C (C/C)	1.00	1.00
H ratio respect to C (H/C)	1.72	1.72
O ratio respect to C (O/C)	0.56	0.56
Bio oil enthalpy of formation [kJ/kmol-C]	-105,354	-105,354
Bio oil sensible heat [kJ/kmol]	26,369	26,375

Parameter	*Unit*	*Coke*
Mass flow rate (dry-mass)	[kg/h]	3.42
HHV dry-mass	[kJ/kg]	33,026
	[kJ/h]	113,015
$H°_f$ combustion product	[kJ/h]	-119,841
$H°_f$	[kJ/h]	-6,826
ΔH (T)	[kJ/h]	3,251

	HGF Output				*Pyrolysis Input*		
	[kg/h]	*kmol/h*	*H (425°C) [kJ/kmol]*	*H(425°C) [kJ/h]*	*[kg/h]*	*kmol/h*	*H(450°C) [kJ/h]*
Bio oil	14.53	0.64	-79,039	-50,379	17.969	0.788	-62,300
Coke	3.42			-3,575			
Total				-62,300			-53,955

Ideal energy requirement for coke formation 8,345 [kJ/h]

3. Fixed Bed Catalytic Upgrading Reactor

Bio oil	*Inlet stream*		*Outlet stream*	
	flow rate (kmol/h)	*Ratio (/C)*	*flow rate (kmol/h)*	*Ratio (/C)*
C	0.79	1.00	0.48	1.00
H	1.35	1.72	0.60	1.25
O	0.44	0.56	0.12	0.25
Bio oil enthalpy of formation [kJ/kmol-C]	-105,354		-35,809	
Bio oil sensible heat at 450°C [kJ/kmol]	26,369		21,045	

Element	*Flue gas product [kmol]*				*$H°_f$ flue gas[kJ/h]*	
	Composition	*$H°_f$ [kJ/kmol]*	*Oil*	*Coke*	*Oil*	*Coke*
C	CO_2	-393,510	0.48	0.03	-188,141	-9,976
H	H_2O	-241,814	0.5	0.04	-72,267	-9,148
	$H°_f$ combustion product				-260,408	-19,124

Parameter	*Unit*	*Coke*
Mass flow rate (dry-mass)	[kg/h]	0.55
HHV dry-mass	[kJ/kg]	33,026
	[kJ/h]	18,034
$H°_f$	[kJ/h]	-1,089
ΔH (T)	[kJ/h]	471

Element	*MW*	*H (425°C) [kJ/kmol]*	*Pyrolysis Output*			*Pyrolysis Input*		
			[kg/h]	*kmol/h*	*H (425°C) [kJ/h]*	*[kg/h]*	*kmol/h*	*H (425°C) [kJ/h]*
CO	28	-98,507	6.739	0.24	-23,708	5.22	0.187	-18,373
CO_2	44	-375,756	11.313	0.26	-96,616	8.77	0.199	-74,873
CH_4	16	-41,196	0.543	0.03	-1,398	0.42	0.026	-1,084
C_2H_4	27	181,451	0.308	0.01	2,094	0.24	0.009	1,622
H_2	2	11,749	0.013	0.01	74	0.01	0.005	57
H_2O (g)	18	-227,622	4.855	0.27	-61,398	3.42	0.190	-43,281
Bio oil			8.267	0.48	-7,059	14.530	0.637	-50,690
Coke			0.546		-619			

Ideal energy released for catalytic upgrading -2,010 [kJ/h]

4. Heat for Drying

Parameters	*exhaust*	*biomass out*	*Air inlet*
T (°C)	60	60	110
mass (kg-dry basis)	1847	40	1847
Moisture (kg)	36.52	3.48	0.00
Water mass fraction	0.02		0
ΔH [kJ/kg db]	83.03		85
ΔH [MJ]	153.33	3.64	156.97

Energy required for drying $1847\frac{kg}{h} \times 1\frac{kJ}{kg.K} \times (110-60)K = 92{,}337\ kJ/h$